

# Graphene in Lithium-Ion/ Lithium-Sulfur Batteries

Guillermina L. Luque<sup>1,\*</sup>, María Laura Para<sup>2</sup>, Emiliano N. Primo<sup>2</sup>,  
M. Victoria Bracamonte<sup>2</sup>, Manuel Otero<sup>1,2</sup>, María del Carmen Rojas<sup>2</sup>,  
Francisco J. García Soriano<sup>2</sup>, German Lener<sup>2</sup> and Andrea Calderón<sup>2</sup>

<sup>1</sup>INFIQC, Departamento de Química Teórica y Computacional, Facultad de Ciencias Químicas, Universidad Nacional de Córdoba-CONICET. Córdoba, Argentina

<sup>2</sup>IFEG, Facultad de Matemática, Astronomía, Física y Computación, Universidad Nacional de Córdoba-CONICET. Córdoba, Argentina

---

## Abstract

In order to deal with the energy demand of the increasing global population, the use of sustainable sources of energy has become mandatory to attenuate the environmental problems that come along with the use of fossil sources of energy. However, one of the problems of renewable energy sources, such as wind or sun, is that they are intermittent. So, in order to make the best use of them, we need good energy storage systems able to capture, manage and store energy at a large scale and low cost. If we are also capable of replacing the gasoline powered transportation with electric vehicles, the greenhouse emissions would be significantly reduced. As well, it is necessary a change in the energetic matrix for stationary devices to solve the transport cost and the greenhouse emission provokes for the use of natural gas. Considering this, the major promises to accomplish the needs of high gravimetric, volumetric and power density is given by lithium batteries. In the past decades and up to nowadays, they have become the energy source of almost all electronic portable devices and made possible a huge number of technological applications. Graphene based materials, due to their unique properties, have become of great interest to be used in different components of the battery: anode, cathode and separator. As part of the electrodes, used adequately, graphene materials improve the electron and ionic mobility providing not only higher electrical conductivity, but also higher capacity. Due to the rich carbon chemistry,

---

\*Corresponding author: gluque@fcq.unc.edu.ar

graphene can be easily functionalized with different groups leading to changes in its properties. In this sense, the nano-sized dimension and elevated specific surface area makes it a perfect candidate for improving conductivity, connectivity and lithium-ion transport in both cathode and anode active materials. Functionalized graphene is also used in the modification of separators of lithium-sulfur batteries for the suppression of the “polysulfide shuttle mechanism” due to its interaction/repulsion with the charged intermediate polysulfide species. This chapter presents a critical overview of the state-of-art in the optimization and application of graphene derived materials for anodes, cathodes and separators in lithium batteries. Besides a thorough description of novel designs and general discussion of the attained electrochemical performances, this chapter also aims to discuss desired properties and current drawbacks for massive industrial application in lithium batteries.

**Keywords:** Graphene, lithium batteries, anode, cathode, separator, functionalized graphene

## 8.1 Introduction

Batteries are devices that store chemical energy to be transformed into electrical energy. They can be divided in two general groups: primary batteries, that commonly are discharged once and discarded afterwards; and secondary or rechargeable batteries, that can be charged and discharged several times depending on their cycle life.

Generally speaking, the batteries are made of one or more power-generating compartments named cells. Each cell is composed of two electrodes, a cathode (positive electrode) and an anode (negative electrode), separated by a non-electronic (blocking electrons inside conductive battery) but ionic conductive film. A battery is a package of one or more galvanic cells used for the production and storage of electric energy by chemical means. A galvanic cell consists of at least two half cells, a reduction cell and an oxidation cell. Chemical reactions in the two half cells provide the energy for the overall galvanic cell operation. Each half cell consists of an electrode and an electrolyte solution. Usually the solution contains ions derived from the electrode by oxidation or reduction reaction. All of these parts are immersed in an electrolyte that allows the mobility of ions leading to a battery voltage potential build up between the two electrodes. The general goal for battery development is to increase energy and power densities, while minimizing volumetric and mass constraint.

Nowadays, lithium-based batteries are the most important storage system available in the market used mainly in portable electronic devices,

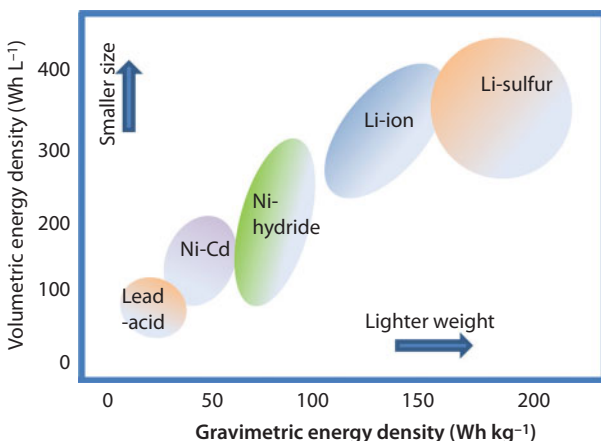


**Figure 8.1** Comparison of volumetric and gravimetric energy density of different types of batteries. The arrows indicate the direction of development to reduce battery size and weight.

electric vehicles (BEVs) and smart grid to storage energy from renewable sources such as sun and wind [1–3]. This is due to the high energy density they possess: a typical lithium-ion battery stores around  $150 \text{ Wh kg}^{-1}$ . In contrast, Ni-hydride (NiMH) can store 60 to 70 and a lead-acid battery can store only  $25 \text{ Wh kg}^{-1}$  as can be seen in Figure 8.1. Besides, they only lose 5% of its charge per month in comparison with 20% loss of NiMH [4]. Also Li batteries have no memory effects, meaning that is not necessary to completely discharge/charge them; and can be charged and discharged hundreds of cycles [5]. Lithium batteries also have higher operation voltages, broader temperature range and lower maintenance requirements than other type of batteries.

The basis of the operation of any electrochemical battery is the movement (diffusion and migration) of charged particles due to an energy difference between the electrodes that store these particles. In the case of lithium batteries, these particles are the lithium ions that circulate inside the battery and react on the electrodes, and the electrons that are produced in those reactions and circulate through the external circuit of the battery. On the diffusion and migration of charged particles the driving force are the concentration gradient and the electric field potential difference, respectively.

At the interfaces between the electrodes and the electrolyte, where there are large differences in the concentration of the mobile charge carriers, is where the drop of the electrostatic potential occurs. An electric

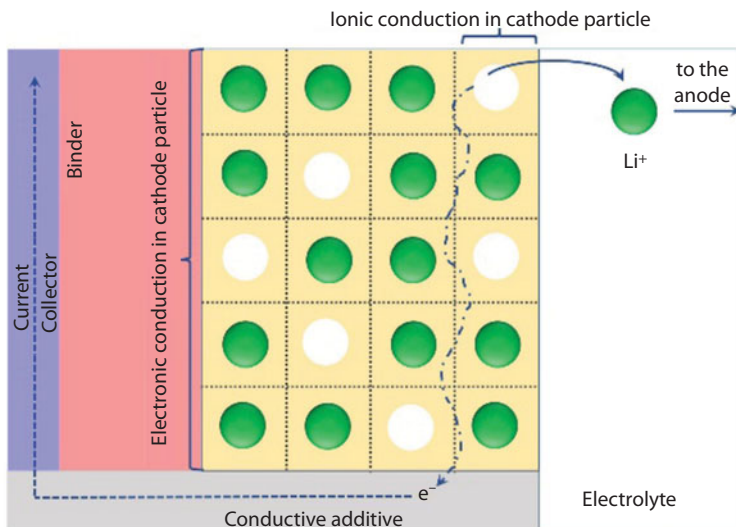


Figure 8.2 Scheme of charge carrier's diffusion on the cathode side of a Lithium Battery.

field is formed to compensate the diffusion of both, electronic and ionic charge carriers. In this case, the main driving force of the ions is the electric field. Even though, the transport originates a concentration gradient. Figure 8.2 shows how charge carriers (electron and lithium ion) move when a positive polarization during charging is applied to a cathode particle: electrons move through the material and conductive additive up to the current collector; at the same time  $\text{Li}^+$  ions moves through cathodic material, and are transferred to the electrolyte and transported through the liquid media up to the anode. The overall process involves also solid state diffusion of charged particles, charge transfer at several interphases and ionic transport on the electrolyte. Because of the above mentioned potential drops, operating potential of the cell ( $E$ ) is lower than standard cell voltage ( $E_0$ ). Mathematically this is:

$$E = E_0 - [(\eta_{ct})_a + (\eta_{ct})_c] - [(\eta_c)_a + (\eta_c)_c] - iR_i = iR$$

where  $(\eta_{ct})_a$ ,  $(\eta_{ct})_c$ ,  $(\eta_c)_a$  and  $(\eta_c)_c$  are activation polarization (charge transfer) and concentration polarization at anode and cathode respectively,  $i$  is the operating current,  $R_i$  is the internal resistance and  $R$  the apparent resistance of the cell [6]. Activation polarization is related to charge transfer kinetic, concentration polarization to mass transport and internal resistance is affected by the conduction properties of the materials and their interfaces [7, 8]. From the equation it is clear that to improve the

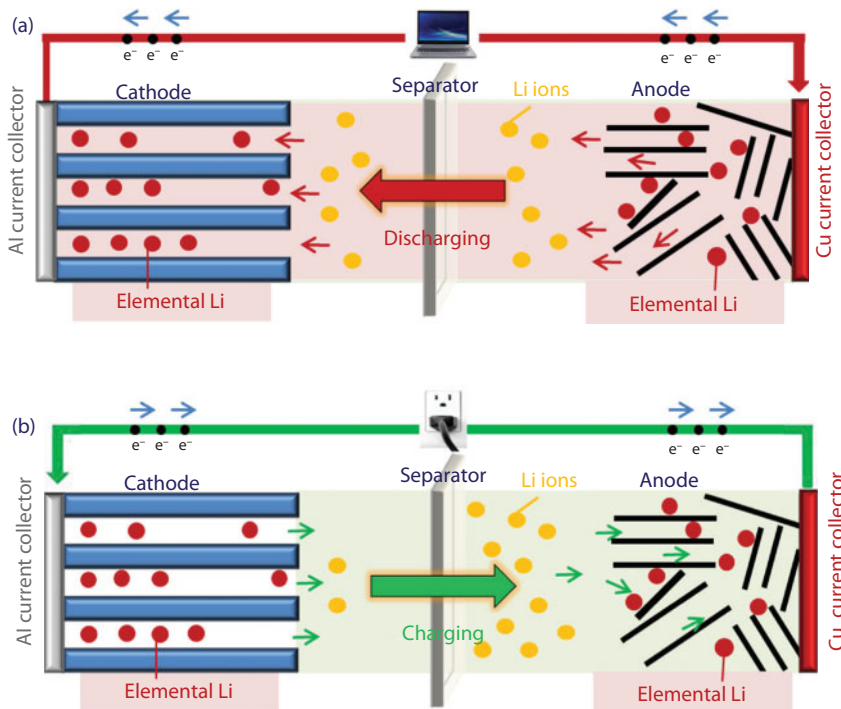


Figure 8.3 Discharging (a) and charging (b) of a lithium battery.

battery's energy efficiency the conductivities and lithiation potentials of all cell components are crucial.

During cycling, lithium ions move back and forth between anode and cathode and through the ionically conducting electrolyte in a “reversible” electrochemical reaction during electron transfer inside and outside the battery. When the battery is discharging and providing current, the anode releases lithium ions to the cathode, generating a flow of electrons from one side to the other (Figure 8.3a). When the device is plugged in (charging) lithium ions are released by the cathode back to the anode (Figure 8.3b). In the first cycles a Solid-Electrolyte-Interphase (SEI) is formed on the surface of the electrodes. The layer formed consists of insoluble and partially soluble reduction products of electrolyte components that acts as an high electronic resistivity interphase between the electrodes and the electrolyte; SEI is the key factor which determines the safety, power capability, cycle life of the battery [9].

The charging and discharging of the battery can be performed at different C-rates. C-rate is the measure of the rate at which a battery is discharged

relative to its maximum capacity. Considering this, 1C rate means that the battery will discharge its current in 1 h. As an example, if a battery has a capacity of 100 Amperes-hour (Ah) this means that the battery would discharge 100 A in one hour [10].

In order to produce a battery with high capacity and high power density, increased safety, fast C-rates, and good cyclability; it is necessary to have good performance lightweight active materials, high conductivity and high surface area. Many of these requirements are attained by graphene.

Graphene is a bi dimensional layer of carbon atoms bonded in a  $sp^2$  configuration forming a honeycomb structure. This material has attracted a lot of interested since it was first discovered by Novoselov and Geim [11] and further applied in many fields due to its high theoretical surface area, high mechanical flexibility, good electrical conductivity and high theoretical capacitance [12]. All these characteristics make graphene a highly promising material to be used in the field of lithium batteries [13–16]. Graphene presents the advantages of having a wide potential window and a great surface versatility allowing the use of this material on its own, or forming hybrids with other cathode and anode materials enhancing the overall electrochemical performance. Its introduction in the cathode or anode enhances the conductivity improving the electron transport and the rate capability of the electrodes along with amelioration in the cyclic stability due to graphene's good mechanical properties. The advantages, drawbacks and limitations of using graphene in cathodes and anodes of lithium-ion, and lithium-sulfur batteries are summarized in this chapter.

## 8.2 Graphene in Lithium-Ion Batteries

In the field of lithium-ion batteries, graphene present the advantage of having a wide potential window and its great surface versatility for functionalization acting as building block for obtaining different materials. At the same time, its high conductivity and layered structure makes this material a good matrix to form hybrids with anodes and cathode materials. These hybrid materials can enhance the electrochemical performance of the final material increasing the conductivity, the electron transfer and the mechanical properties [17–19]. This is a very important fact in order to promote the development of new electrode structures and new types of lithium-ion batteries (LIBs).

Actual LIBs consist mainly of graphite as anode electrode by intercalating Li ions reversibly in the interlayer spaces and a lithium-ion intercalation

material as a positive electrode (usually lithium metal oxide) separated by an ion conductive but electrical insulation separator immersed in an ion conducting organic electrolyte [4]. However, due to miniaturization and to their use in new different applications such as aerospace, military and automotive applications new materials are necessary in order to achieve the needs of high performance devices (increasing their mass capacities ( $\text{Whkg}^{-1}$ ), and their energy densities ( $\text{WhL}^{-1}$ ) [1, 1, 16, 20]. Graphene with its properties can serve to enhance the overall electrochemical performance of the lithium-ion battery.

### 8.2.1 Graphene in Anodes of Lithium-Ion Batteries

The first commercialized Li-ion batteries, introduced by Sony in 1991, used graphite as anode material and  $\text{LiCoO}_2$  as cathode [21]. Although several improvements have been made in the positive electrode by using different materials [22] the commercial negative electrode is still based on graphite. The next energy revolution requires the replacement of internal combustion vehicles by full-electric vehicles. To this purpose, LIB arises as the most promising storage system [23]. However, current graphite-based LIB technology has low autonomy range, long charging time and high costs, compared with internal combustion vehicles, therefore demanding an improvement of its storage system. In this context, due to the great scientific community excitement around graphene and its derived materials, these materials were initially proposed as graphite-next-generation anode material for LIBs.

In this sense, therefore, two configurations were early proposed which circumvent the limitation of graphite's  $\text{LiC}_6$  maximum lithiated phase: one is the double layer adsorption and another is the covalent molecule configuration. In the first case [24], both planes of a graphene sheet adsorb Li ions, yielding  $\text{Li}_2\text{C}_6$  with a specific capacity of  $\sim 780 \text{ mAh g}^{-1}$ . In the latter case [25], each Li atom is trapped at a covalent site on the benzene ring and therefore the highest Li storage capacity of  $\sim 1116 \text{ mAh g}^{-1}$  corresponding to  $\text{LiC}_2$ . Initial work by Yoo *et al.*, [26] aimed to study lithiation/delithiation behaviour of reduced graphene oxide (RGO) synthesized through Hummer's method and reduced with hydrazine. They found that in the charging (lithiation) curve, the slope starts at  $\sim 2.50 \text{ V}$  (vs  $\text{Li}/\text{Li}^+$ ) and has large specific capacity below  $0.50 \text{ V}$  without distinguishable plateaus. Although initial capacity was  $540 \text{ mAh g}^{-1}$  (cycling at  $0.05 \text{ A g}^{-1}$ ), after 20 cycles it fades up to  $290 \text{ mAh g}^{-1}$ . Subsequent research efforts were made focusing in RGO as anode material. An analysis of lithium uptake properties with reduction strategy on RGO [27] showed that specific capacity

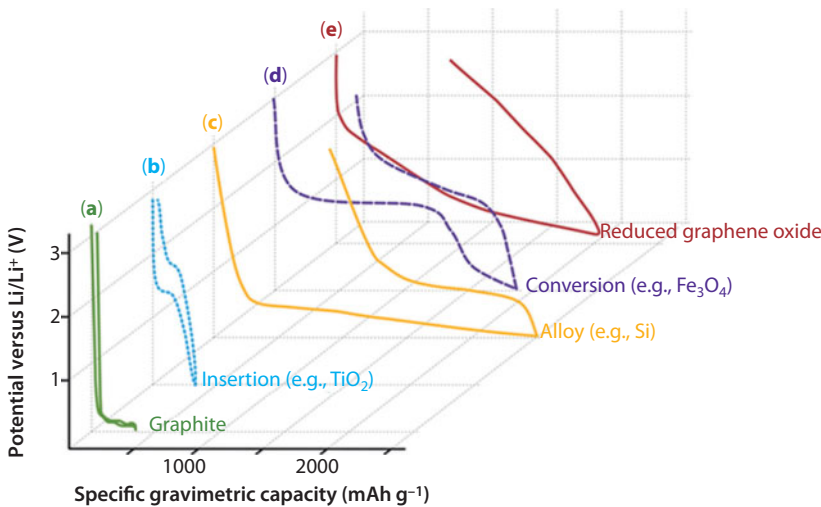


**Figure 8.4** Comparison of typical voltage profiles of lithium-ion battery anode materials: (a) Li intercalation into graphite, (b) insertion of Li in high voltage oxides (e.g.,  $\text{TiO}_2$ ), (c) materials forming alloying with Li (e.g., Si), (d) materials undergoing conversion reactions with Li (e.g.,  $\text{Fe}_3\text{O}_4$ ), and (e) Li storage in reduced graphene oxide.

ranged from 200, 830, 640 and 740  $\text{mAh g}^{-1}$  for hydrazine, 300 °C and 600 °C thermally, and electron beam-reduced (after 15 cycles at 0.050  $\text{A g}^{-1}$ ). Other groups reported quite different behaviour such as 120  $\text{mAh g}^{-1}$  for thermally expanded RGO (100 cycles at 0.004  $\text{A g}^{-1}$ ) [28], 338  $\text{mAh g}^{-1}$  for 500 °C thermally-RGO (50 cycles at 0.050  $\text{A g}^{-1}$ ) [29] or as high as 872 and 1227  $\text{mAh g}^{-1}$  for N-doped and B- doped RGO, respectively (30 cycles at 0.050  $\text{A g}^{-1}$ ) [30]. Following such high capacities attained by doping graphene with heteroatoms, several research focused in this area and a high number of reports were made using N-doped [31–33], S-doped [34, 35], P-doped [36] or even co-doped [37, 38] graphene materials.

Despite the initial scientific excitement towards graphene-derived materials, mainly between 2010 and 2014, none of the above proposed strategies succeeded to overcome the two main disadvantages: high initial capacity fading and plateau-less potential profiles (Figure 8.4). Graphene-derived materials generally show a first irreversible capacity loss, which can be as high as 85% and it greatly depends on the synthesis method [39–41]. The second drawback is associated to the sloppy and steep voltage profiles (showing no plateaus at all) and a discharge capacity delivered mostly at potentials of 1–3 V (versus  $\text{Li}/\text{Li}^+$ ) leading to large voltage hysteresis upon insertion and de-insertion of  $\text{Li}^+$ , which results in poor energy efficiency for cells employing such electrodes [42, 43]. These features come

from the presence of many kinds of oxy-functional groups and defects as a consequence of the widely used top-down synthesis methods [44–47]: Hummer's, liquid-phase exfoliation or electrochemical/chemical expansion of the sheets. In 2014, Robledo *et al.*, [48, 49] analysed through density functional theory (DFT) calculations, the lithium binding energy of graphene sheets functionalized with several –OH, =O and epoxy groups. They found that lithiation potential increases with the degree of oxidation of graphitic sheets, as strong covalent interaction is formed between Li and O rather than between Li and C, confirmed through PDOS calculations. Other authors also showed the dependence of Li-ion diffusivities along graphene sheets with its defects and diffusion direction [50]. Through DFT calculations and experimental evidences, they concluded that di-vacancies and higher order defects have reasonable diffusion barrier heights allowing lithium diffusion through the basal plane while high barriers were expected for mono-vacancies and Stone-Wales defect. Furthermore, diffusion along the basal plane is sterically hindered as lithiation proceeds. Comprehensive work done by Yakobson's [51] and Kostecki's [52] groups demonstrated that the strong Coulombic repulsion of  $\text{Li}^+$  facing opposite sides of a single graphene sheet results on lower binding energies, likely leading to a very low surface coverage. In this case only the formation of Li clusters is favoured, against full-layer intercalation/adsorption, therefore excluding the possibility of existence of the so-called  $\text{Li}_2\text{C}_6$  and  $\text{LiC}_2$  phases.

As explained above, when graphene is used as bare active material, it does not show any benefits as opposed to conventional graphite or other anode active materials. Another disadvantage of these kinds of materials is its high specific area, which makes its volumetric capacity even lower than graphite. Nonetheless, its efficiency to adsorb almost to any kind and shape of materials and its highly conductive nature (when properly synthesized) has proven a successful choice as additive to other insulate active materials for anodes in LIB.

The addition of graphene to other lithium electroactive materials, such as metal (or metal oxide) nanoparticles, provides reversible alloying ( $\text{Sn}$ ,  $\text{SnO}_2$ ,  $\text{Si}$ ,  $\text{Ge}$ ), insertion ( $\text{Li}_4\text{Ti}_5\text{O}_{12}$ ,  $\text{TiO}_2$ ) or conversion ( $\text{M}_y\text{O}_x$ , with  $\text{M}$  a transition metal) reactions with lithium, thus allowing considerably higher storage capacities than those of bare graphene or active materials [20, 42, 43]. During the composite preparation, graphene acts as a support for the growth of electroactive structures also aid in preventing the re-stacking/re-agglomeration during electrode preparation, as well as in preventing the capacity fading during cycling. Moreover, the extensive and highly conductive carbon matrix established by graphene layers improves

the electrical conductivity of the composite and buffers eventual volume changes taking place in electrodes based on alloying or conversion materials during cycling [17, 53, 54].

The most common alloying-type anode materials Si, Ge and Sn are semiconductor materials that present considerable higher capacities (3579, 1384 and 960 mAh g<sup>-1</sup>, respectively) [55] but have poor cycling performance [56]. In particular Ge has a production cost ~ 1000 times higher than Si and Sn, making it commercially unfeasible [57]. The lithium alloys formed by these materials during the charge generates volume changes higher than 250% [55]. This expansion/contraction cycles damage the electrode internal structure leading to problems in electric contact and high electrolyte consumption due to the continuous SEI formation, which reflects in a reduction of capacity upon cycling.

Graphene has been widely implemented in combination with active Si nanostructures [58–61]. Different methods of coating Si nanoparticles (SiNPs) by graphene have delivered promising candidates for LIBs [62, 63]. Particle morphology of Si active material is of paramount importance for extended cyclability of these kinds of anodes. In this sense, mechanical stress due to huge volume expansion of Si-based anodes has been alleviated by introducing hollow spaces into SiNPs, coating them with conductive layers or generating yolk-shell structures [62, 64, 65]. Lee *et al.*, [66] presented a SiNPs/graphene composite fabricated by filtering Si/graphene oxide mixes and further subject them to thermal reduction. This material showed a reversible capacity of 1500 mAh g<sup>-1</sup> after 200 cycles, which decreased less than 0.5% per cycle. In another application, Zhou *et al.*, uniformly encapsulated SiNPs in graphene via a self-assembly approach based on electrostatic interactions [67]. The composite presented a very stable cycling behaviour with a capacity of ~1200 mAh g<sup>-1</sup> up to 150 cycles. Spin coating technique was used by Zhou *et al.*, [68] to construct SiNPs/graphene anodes with a high capacity of 1611 mAh g<sup>-1</sup> after 200 cycles at 1 A g<sup>-1</sup>, and good rate capability of 648 mAh g<sup>-1</sup> at 10 A g<sup>-1</sup>. The presence of graphene as support/coating also promotes Si-based anodes cyclability which is one of the main drawbacks that prevents its widespread application. Wang *et al.*, used silicon nanowires wrapped within hollow tube-like graphene sheets [69]. This void-incorporated one-dimensional material delivered good rate capability (1200 mAh g<sup>-1</sup> at 12.60 A g<sup>-1</sup>) and remarkable cycling stability (1100 mAh g<sup>-1</sup> at 4.20 A g<sup>-1</sup> over 1000 cycles) when used as anode. In another report, Hassan *et al.*, [70] proposed a hybrid concept that capitalized on the strong covalent interactions occurring between SiNPs and sulfur-doped graphene (SG) as well as cyclized polyacrylonitrile (cPAN). DFT calculations on the mobility of adsorbed Li indicated its

diffusion on SG-Si with a slightly lower barrier than that found on normal graphene-Si, disclosing that SG could boost the mobility for lithium atoms on Si-SG interface [70]. The thus-fabricated Si-SG-cPAN electrode exhibited a high coulombic efficiency of 99.9% and superior reversible capacity of over 1000 mAh g<sup>-1</sup> for 2275 cycles at 2.00 A g<sup>-1</sup>. Likewise, the work of Zhao *et al.*, [59] showed that graphene having a high density of defects and vacancies can contribute as a flexible, 3D conducting scaffold with abundant cross-plane paths for Li ion diffusivity and great tolerance to mechanical deformation. Urquiza *et al.*, [71] used DFT calculations to determine the interaction of small Si cluster on defective graphene. They demonstrated that a relatively small amount of defects and vacancies in graphene structure generates a very strong Si-C adhesion. They also found that the deposition of Si atoms on vacancies increases the density of states in the Fermi level, improving the conductivity of the system.

The use of graphene to stabilize Sn active nanostructured anodes has also been addressed by several research groups [72, 73]. The optimization of Sn nanoparticles (SnNPs) combined with graphene have deliver great electrode performance reaching over 838 mAh g<sup>-1</sup> after 100 cycles [74]. It has been found that the SnNPs size has a huge effect on the final composite electrode properties. In the report of Wang *et al.*, [75] a microwave hydro-thermal synthesis was used to obtain SnNP of different sizes, showing that the ones with smaller diameter (10–20 nm) surpass the capacity of the larger ones (40–60 nm). It is suggested that the reduced particle size effectively decrease the pulverizations and cracking due to volume changes and graphene helps to maintain a correct connectivity [76]. Moreover, smaller particle sizes significantly increase the charge/discharge rates, because of the short distances for lithium-ion transport inside the semiconductor. The use of graphene in Sn-based anodes has also been reported to facilitate Li<sup>+</sup> charge transfer. The sandwiching of Sn particles hydrothermally synthesized at RGO/carbon nanotube mixture exhibited capacities as high as 1160–982 mAh g<sup>-1</sup> (100 cycles at 0.10 Ag<sup>-1</sup>) and excellent rate capability (828 mAh g<sup>-1</sup> at 1.00 A g<sup>-1</sup> and 594 mAh g<sup>-1</sup> at 5.00 A g<sup>-1</sup>) [77]. The formation of complex graphene based architectures also increases the cyclability, as in Qin *et al.*, work [74] where SnNPs (5–30 nm) encapsulated with graphene shells showed a 96.3% of capacity retention after 1000 cycles at 2.00 A g<sup>-1</sup> (specific capacity of 682 mAh g<sup>-1</sup>). Similar electrodes where prepared combining graphene with SnO<sub>2</sub> as active material [78], which present an exceptional cycling stability up to 2000 cycles [79].

Spinel Li<sub>4</sub>Ti<sub>5</sub>O<sub>12</sub> (LTO) has been studied extensively and is considered as one of the most promising insertion anode materials for high-power LIBs [80, 81]. LTO anodes exhibit a flat and relatively high redox potential

(1.55 V versus Li/Li<sup>+</sup>), avoiding the formation of solid electrolyte interface and therefore allowing to sustain high current densities as well as to reduce safety issues [81–83]. However, the low electronic conductivity (<10<sup>-13</sup> S cm<sup>-1</sup>) [84] and relatively low Li<sup>+</sup> diffusion coefficient (<10<sup>-13</sup> cm<sup>2</sup> s<sup>-1</sup>) [85, 86] of LTO resulted in an insufficient rate performance lowering its practical application. Initial studies pointed out the improvement in specific capacity and kinetic limitations of LTO by interphacing it with RGO. Nonetheless, and as pointed out before, graphene synthesis method has a huge impact in the effect on LTO as anode enhancement properties therefore leading to different conclusions [87]. Yoon *et al.*, [88] demonstrated that when a nanocomposite is formed using LTO and thermally-RGO, the rate capability is improved owing to a shortening in the distance for Li ion diffusion in the LTO. Therefore, the improved rate capability is ascribed to the enhanced diffusion properties in the bulk particle electrochemical reaction sites rather than an increase in the electrical conductivity, which is a surface property. In LTO/N-doped graphene hybrids in Ding *et al.*, [89] studies, electron transfer from the LTO surface to graphene greatly improves the electric conductivity of the interface, while N-dopants in graphene coatings further increase the interfacial stability and electric conductivity. Therefore, it is clear that the presence of graphene materials improves the capacity retention of LTO while cycling it at high C-rates. The introduction of GO double layers at LTO-nanofibers (NF) hybrids in Kim *et al.*, work [90] prove to enhance rate capability (110 mAh g<sup>-1</sup> at 20 C) and increased in over two orders of magnitude Li diffusion coefficient ( $D_{Li} = \sim 1.04 \times 10^{-11}$  cm<sup>2</sup> s<sup>-1</sup>) compared with pristine LTO-NFs. Ge *et al.*, [91] reported mesoporous LTO-RGO hybrids by glucose-assisted hydrothermal reduction of LTO-GO mixture. At an extremely high 30 C rate, the mesoporous LTO-RGO anode was able to retain 87% capacity measured at 0.5 C (193 mAh g<sup>-1</sup>) with well-defined voltage plateau. Meng *et al.*, work [92] on LTO particles with sizes of 50–100 nm and dispersed homogeneously on a 3D “fishnet-like” graphene architecture showed an excellent cycle performance with 95.4% capacity retention at 10 C after 100 cycles and a high specific capacity of 176.6 mAh g<sup>-1</sup> at 1 C.

### 8.2.2 Graphene Applied to Cathode Materials for Lithium-Ion Batteries

Normally, the materials used as cathodes for LIBs are inorganic compounds with a transition metal cation which can be oxidized/reduced with the consequent deintercalation/intercalation of lithium ion within the crystal's structure. Transition metal compounds are used due to their high oxidation

potential, as it determines the overall potential of the cell. Different families of cathodes can be classified according to their structural geometry and/or chemical type. The principal groups are: (i) layered  $\text{LiMO}_2$ ; (ii) Li-rich layered  $\text{Li}_{1-x}\text{M}_{1-x}\text{O}_2$ ; (iii) spinel  $\text{LiM}_2\text{O}_4$ ; (iv) olivine  $\text{LiMPO}_4$ ; (v) silicate compounds  $\text{Li}_2\text{MSiO}_4$ ; and (vi) borate compounds  $\text{LiMBO}_3$ . Some other cathode materials like fluorides ( $\text{FeF}_3$ ), oxides ( $\text{MnO}_2$ ,  $\text{V}_2\text{O}_5$ ),  $\text{LiV}_3\text{O}_8$  and  $\text{Li}_3\text{V}_2(\text{PO}_4)_3$  have also been studied [93]. These typical cathode materials have a considerable band gap between occupied and conduction electronic bands, which means they have low conductivity. In order to generate high power electrochemical applications it is necessary to increase their electronic and ionic conductivity, as it was previously discussed in order to improve the overall electrode performance.

Several cathodes materials have very low electric conductivity ( $\text{LiCoO}_2$ ,  $10^{-4}$  S cm<sup>-1</sup> [94, 95];  $\text{LiMn}_2\text{O}_4$ ,  $10^{-6}$  S cm<sup>-1</sup> [96, 97];  $\text{LiFePO}_4$ ,  $10^{-9}$  S cm<sup>-1</sup> [98, 99];  $\text{Li}_3\text{V}_2(\text{PO}_4)_3$ ,  $10^{-7}$  S cm<sup>-1</sup> [100]). Different strategies are used to increase electronic conductivity, one of the most common being the combination with some conductive material, preferably carbon because is an electric conductor with low mass specific weight. Conventional carbon additives such as carbon black have lower electronic conductivities compared to more crystalline forms of carbon [101]. In a straightforward way, carbonaceous materials with larger surface/mass ratios will be more efficient for being used as coating [102]. Therefore, graphene derived materials are one of the most suited candidates.

Although most of the studies with graphene are in the development of  $\text{LiFePO}_4$  [103–107] cathodes due to the fact that is the one with lower conductivity and with greater industrially use. There are also studies in other systems based on  $\text{LiMn}_2\text{O}_4$  [108, 109],  $\text{LiCoO}_2$  [110] and  $\text{Li}_3\text{V}_2(\text{PO}_4)_3$  [111–115], which present theoretical electric power density higher than  $\text{LiFePO}_4$ .

Table 8.1 presents some relevant materials employed for cathodes and anchored upon and/or into graphene-derived nanostructures using some different strategies.

$\text{LiFePO}_4$ /graphene hybrids were synthesized using diverse strategies that involves encapsulation [117, 118] or anchoring nanoparticles on graphene derivates [123, 124]. Su *et al.*, [125] have synthesized a  $\text{LiFePO}_4$ /graphene/carbon composite by using an *in situ* solvothermal method to obtain the  $\text{LiFePO}_4$ /graphene powders and then followed by a carbon-coating process. The results indicated that the co-modification enhanced the electrochemical activity of  $\text{LiFePO}_4$ /carbon based composite. Particularly, the composite with a low content of graphene exhibited a high initial discharge capacity of 163.7 mAh g<sup>-1</sup> at 0.1 C and 114 mAh g<sup>-1</sup> at 5 C, as well as an excellent cycling stability.

Table 8.1 Summary of experimental data for different cathode materials.

Material	Synthesis method	Structure	Capacity (C rate) without graphene	Capacity (C rate) with graphene	Ref.
LiFePO <sub>4</sub>	<i>In situ</i> -Solvothermal	Wrapped	141.0 mAh g <sup>-1</sup> (0.1 C) approx 58 mAh g <sup>-1</sup> (5 C)	163.7 mAh g <sup>-1</sup> (0.1 C) 114.0 mAh g <sup>-1</sup> (5 C)	[116]
LiFePO <sub>4</sub>	Solid State reaction	Wrapped	--	166.6 mAh g <sup>-1</sup> (0.1 C) 108.6 mAh g <sup>-1</sup> (5 C)	[117]
LiFePO <sub>4</sub>	Hydrothermal	Anchored	123.7 mAh g <sup>-1</sup> (0.1 C) 30.6 mAh g <sup>-1</sup> (10 C)	160.3 mAh g <sup>-1</sup> (0.1 C) 81.5 mAh g <sup>-1</sup> (10 C)	[118]
LiFePO <sub>4</sub>	ball milling-assisted rheological phase/ solid-state reaction	Sandwich-like	144.5 mAh g <sup>-1</sup> (0.1 C) approx 40 mAh g <sup>-1</sup> (20 C)	160.8 mAh g <sup>-1</sup> (0.1 C) 81.2 mAh g <sup>-1</sup> (20 C)	[119]

(Continued)

Table 8.1 Cont.

Material	Synthesis method	Structure	Capacity (C rate) without graphene	Capacity (C rate) with graphene	Ref.
$\text{LiMn}_{1-x}\text{Fe}_x\text{PO}_4$	<i>In situ</i> -controlled hydrolysis	Anchored	--	155 mAh g <sup>-1</sup> (0.5 C) 132 mAh g <sup>-1</sup> (20 C)	[120]
$\text{LiMn}_2\text{O}_4$	Anchored after separately synthesis	Mixed	130.4 mAh g <sup>-1</sup> (0.1 C) approx 70 mAh g <sup>-1</sup> (6 C)	140.1 mAh g <sup>-1</sup> (0.1 C) approx 85 mAh g <sup>-1</sup> (6 C)	[108]
$\text{LiCr}_{0.05}\text{Mn}_{1.95}\text{O}_4$	Anchored after separately synthesis	Mixed	137.2 mAh g <sup>-1</sup> (0.1 C) approx 78 mAh g <sup>-1</sup> (6 C)	140.2 mAh g <sup>-1</sup> (0.1 C) approx 90 mAh g <sup>-1</sup> (6 C)	[108]
$\text{LiMn}_2\text{O}_4$	Anchored after separately synthesis	Anchored and sandwich like	126 mAh g <sup>-1</sup> (0.5 C) 36 mAh g <sup>-1</sup> (20 C)	136 mAh g <sup>-1</sup> (0.5 C) 90 mAh g <sup>-1</sup> (20 C)	[121]
$\text{Li}_3\text{V}_2(\text{PO}_4)_3$	Sol-gel Method	Wrapped	106.6 mAh g <sup>-1</sup> (0.2 C)	122.3 mAh g <sup>-1</sup> (0.2 C) 80.2 mAh g <sup>-1</sup> (20 C)	[122]

(Continued)

Table 8.1 Cont.

Material	Synthesis method	Structure	Capacity (C rate) without graphene	Capacity (C rate) with graphene	Ref.
$\text{LiCoO}_2$	Mechanical mixing after separately synthesis	Mixed	146 mAh g <sup>-1</sup> (1 C) 112.3 mAh g <sup>-1</sup> (5 C)	146 mAh g <sup>-1</sup> (1 C) 116.5 mAh g <sup>-1</sup> (5 C)	[110]

Moreover, Xu *et al.*, [126] synthesized encapsulated  $\text{LiFePO}_4$ /graphene composite by solid state reaction using  $\text{FeOOH}$  as starting material. The authors obtained  $\text{LiFePO}_4$  nanoparticles, of 20 nm average size, wrapped tightly within a 3D graphene network. Such a special nanostructure facilitated the electron and lithium ion migration to provide good electrochemical performance, especially at high current rates. This material delivered discharge capacities of 166.6, 108.6 and 90.6  $\text{mAh g}^{-1}$  at 0.1 C, 5 C and 10 C respectively. Also, these structures showed a capacity decay of only 9% when cycled 300 times at 5 C and 10 C.

In another study, Wang *et al.*, [123] prepared a  $\text{LiFePO}_4$ /graphene composite through a facile hydrothermal route followed by a thermal treatment. It was found that the  $\text{LiFePO}_4$  particles are adhered to the surface of graphene and/or embedded in the graphene nanosheets. As a result, an effective three-dimensional conducting network was formed by bridging graphene nanosheets, which can facilitate the effective electron transport and thus improve the kinetics and rate performance of  $\text{LiFePO}_4$ . The  $\text{LiFePO}_4$ /graphene (92:8 wt.%) composites exhibited a discharge capacity of 160.3  $\text{mAh g}^{-1}$  at 0.1 C and 81.5  $\text{mAh g}^{-1}$  at 10 C, respectively. The comparative investigation on  $\text{LiFePO}_4$ /graphene composites and  $\text{LiFePO}_4$  proved that establishing a mixed conducting network with graphene has the potential to enhance the specific capacity and rate capability of  $\text{LiFePO}_4$ . Recently, Wang *et al.*, [127] prepared nano-hybrids of graphene-decorated carbon-coated  $\text{LiFePO}_4$  nanospheres using a ball milling-assisted rheological phase method combined with a solid-state reaction. The synthesized composite exhibited a multilayer graphene film decorated with  $\text{LiFePO}_4$  nanospheres without stacking. This resulted in an abundance of mesoporous constituting a unique 3D “sheets-in-pellets” and “pellets-on-sheets” conducting network structure. As a result, the hybrids with approximately 3 wt% graphene exhibited an outstanding rate capability with an initial discharge capacity of 163.8 and 147.1  $\text{mAh g}^{-1}$  at 0.1 C and 1 C, and the capacity was retained at 81.2  $\text{mAh g}^{-1}$  even at 20 C. Moreover, the composites also revealed an excellent cycling stability with only an 8% capacity decay at 10 C after 500 cycles.

Other types of metal oxides used as cathodes for LIBs are based on partial or total substitution of Fe with others transition metals to generate lithium transition-metal phosphates  $\text{LiMPO}_4$  (M = Fe, Mn, Co, V, or Ni) with olivine type crystallographic group. In this sense, compared to  $\text{LiFePO}_4$ ,  $\text{LiMnPO}_4$  is an attractive cathode material owing to its higher  $\text{Li}^+$  intercalation potential of 4.1 V versus  $\text{Li}/\text{Li}^+$  (3.4 V for  $\text{LiFePO}_4$ ), providing ~ 20% higher energy density than  $\text{LiFePO}_4$  for LIBs [128–132]. Wang *et al.*, presented a two-step approach for the synthesis of  $\text{LiMn}_{1-x}\text{Fe}_x\text{PO}_4$

nanorods on reduced graphene oxide sheets. Fe-doped  $Mn_3O_4$  nanoparticles were first selectively grown onto graphene oxide by controlled hydrolysis. Then, the oxide nanoparticle precursors reacted solvothermally with Li and phosphate ions and were converted into  $LiMn_{1-x}Fe_xPO_4$  on the surface of reduced graphene oxide. Thus, the resulting hybrid of nanorods and graphene showed high specific capacity. Some stable capacities of 132 mAh g<sup>-1</sup> and 107 mAh g<sup>-1</sup> at high discharge rates of 0.5 C and 50 C were obtained, which is 85% and 70% of the capacity at 0.5 C (155 mAh g<sup>-1</sup>), respectively. This leaves the door open to LIBs cathode with both high energy and high power densities [120].

Other types of materials used for high power LIBs are based in metal transition oxides as  $LiMn_2O_4$ /graphene and materials with substitutions in the crystallographic site of the transition metal. Guler *et al.*, [108] proposed a graphene/ $LiMn_2O_4$  (G/LMO) and graphene/ $LiCr_{0.05}Mn_{1.95}O_4$  (G/LCMO) free-standing composite cathode electrodes with increased specific capacity and improved electrochemical capability. Spinel LMO nanorods were synthesized by calcination method followed by a hydrothermal reaction. After that, the synthesized nanorods were then embedded in a graphene layer. For G/LCMO samples, a discharge capacity of 114.5 mAh g<sup>-1</sup> was obtained after the first cycle and 72% of the capacity was retained after 250 cycles. The enhancement in the electrochemical properties was attributed to the unique freestanding structure of the cathode electrodes. Luo *et al.*, [121] successfully prepared  $LiMn_2O_4$ /graphene by mixing spinel  $LiMn_2O_4$  particles with reduced graphene oxide. The results showed an improvement of the electrochemical properties compared to  $LiMn_2O_4$  without graphene [133]. The discharge capacity was 131 mAh g<sup>-1</sup> and the capacity remains at 89.3% after 100 cycles at 0.5 C rate, while the discharge capacity was 90 mAh g<sup>-1</sup> at 10 C.

Another kind of cathode active material used to increase the energy and power densities of LIBs is monoclinic  $Li_3V_2(PO_4)_3$ . Yang *et al.*, [122] fabricated a composite of  $Li_3V_2(PO_4)_3$  NPs/RGO through a sol-gel method. The discharge capacity of the  $Li_3V_2(PO_4)_3$  NPs/RGO was 122.0 mAh g<sup>-1</sup> in the 1<sup>st</sup> cycle at a current density of 140 mA g<sup>-1</sup>, with a capacity retention rate of 97% after 100 cycles. Even cycling at high current density (20 C), the capacity retention was as high as 89.5% after 500 cycles. The excellent cycling performance and rate capability was attributed to the presence of RGO surrounding  $Li_3V_2(PO_4)_3$  NPs, which improved the electrical conductivity and suppressed the aggregation of the  $Li_3V_2(PO_4)_3$  NPs during the cycling.

The gold-standard cathode material  $LiCoO_2$ , has poor electric conductivity ( $10^{-3}$  S cm<sup>-1</sup>). As previous cases, the addition of graphene structures

have been one of most used strategies to improve the electric conductivity. In the case of micro-sized  $\text{LiCoO}_2$  system, the graphene additive does not present hindrance effect for lithium ion transport even at high rate discharge, which is entirely different from the nano-sized  $\text{LiFePO}_4$  system. Tang *et al.*, [110] demonstrated that a low amount of graphene sheets can provide an effective conductive network, which exhibits outstanding cycling stability (146  $\text{mAh g}^{-1}$  at 1 C with retention of 96.4% after 50 cycles) and rate capability (116.5  $\text{mAh g}^{-1}$  even at 5 C).

In general, graphene is added as conductive additive to cathodic material particles for an improvement on electrochemical behaviour since graphene/metal oxide can form a 3D conducting network. However, there is experimental evidence pointing out that, if too much graphene is added the electrochemical behaviour is worse than without it, showing higher polarizations and smaller capacity for high C rates [102]. Opposite to this, if other carbon material (as carbon black or graphite) is used, the electrochemical behaviour gets better with higher amounts of carbonaceous material [134]. Why is the battery performance reduced when bigger amounts of graphene are added if it theoretically improves the electronic conductivity? The answer relies on the ionic conductivity, which is the rate-controlling step of the overall process. In this sense, graphene sheets block  $\text{Li}^+$  ion transport because  $\text{Li}^+$  cannot pass through its planar structure. So, when a  $\text{Li}^+$  ion diffuse through the electrode structure, each time it reaches a graphene layer it must find a not blocked path. This results in an increase of tortuosity for ions path between cathode material and

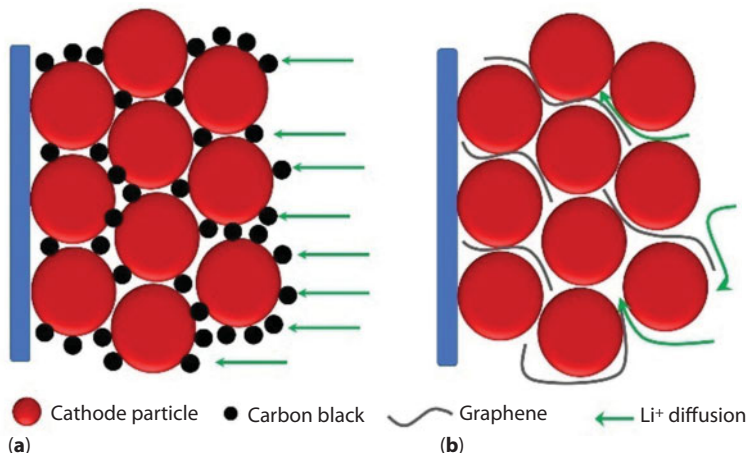


**Figure 8.5** (a) Schematic of  $\text{Li}^+$  transport on cathode with a) carbon black particles, (b) graphene layers.

electrolyte, as is schemed in Figure 8.5 [93, 102]. For example, Su *et al.*, [102] found that when graphene is added to a cathodic material, the capacity increases by 10% at 0.5 C. For higher C rates (1 to 4 C) not only the capacity is decreased by around 40% when compared to the cell without graphene at 3 C, but also a high polarization is observed. This polarization effect is related to the tortuosity-driven deficiency of lithium ions at the reacting interphase which produces an increase of the electric field to compensate the difference on concentration of ions [135, 136].

### 8.3 Graphene in Lithium-Sulfur Batteries

Lithium-sulfur batteries consist mainly in a metallic lithium anode and a cathode with sulfur as active material. Even though they were patented in early 1962 [137], its low rate capability, due to the insulating nature of S and  $\text{Li}_2\text{S}$ , and fast capacity fading, due to the polysulfide shuttling mechanism, prevent them to be applicable up to now [138].

When technical and economic considerations are combined, current projections suggest that BEVs (battery electric vehicles) using state-of-the-art Li-ion batteries may not be able to exceed a range of 200 miles for the mid-size car market [139]. For that reason, advanced electrode materials

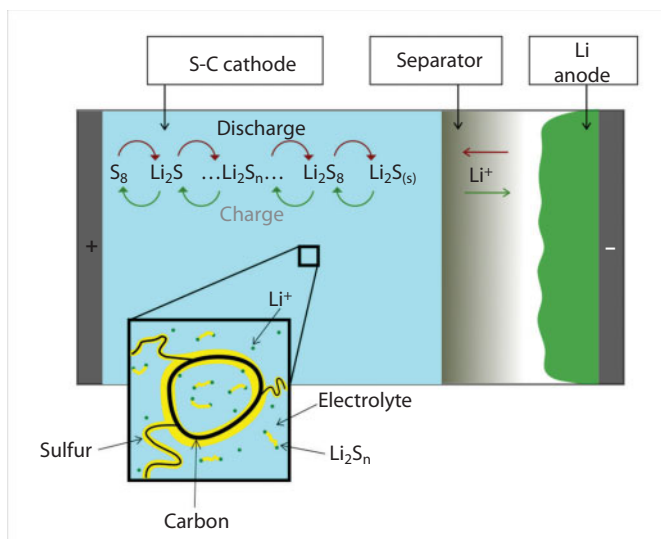


**Figure 8.6** Graphical representation of the polysulfide formation and shuttle effect affecting Li-S cathodes.

are critically demanded to further enhance the energy/power density of next-generation lithium batteries. Therefore, research on post LIB technologies such as lithium-sulfur (Li-S) batteries have received increasing attention [140].

As a cathode material, sulfur offers a theoretical gravimetric capacity of  $1675 \text{ mAh g}^{-1}$  [140, 141], which is six times the theoretical gravimetric capacity of actual NMC (Lithium Nickel Cobalt Manganese Oxide,  $278 \text{ mAh g}^{-1}$ ) LIB cathodes [142]. Additionally, sulfur is a promising material since it is abundant, inexpensive and non-toxic. To date, however, Li-S batteries are not too much commercialized [143]. Their high theoretical energy density is decreased by the need of a conductive carbon support to compensate for the insulating nature of sulfur and the volume change during cycling. Additionally, the realization of a lithium metal anode is problematic due to safety concerns [144].

A recent evaluation estimates that Li-S batteries might, realistically, not exceed the energy density of LIB but be advantageous in terms of lower cost and reduced environmental impact [144–146]. Nevertheless, as the commercial realization of Li-S batteries would accelerate the progress in lightweight energy storage, it is important to improve their cell chemistry. Instead of the intercalation mechanism that take place in LIB, Li-S batteries cathodes undergo a conversion reaction to form  $\text{Li}_2\text{S}$  during discharge and  $\text{S}_8$  during charge through a series of both chemical and electrochemical reactions as can be seen in Figure 8.6. During the operation of the battery, intermediate polysulfide species can be dissolve in the electrolyte and diffuse throughout the battery. Once the polysulfides reach the anode they irreversibly react with metallic lithium, passivating it and forming “dead” sulfur containing species [147, 148] degrading the performance of the battery. These soluble intermediates have been held responsible for major drawbacks of the system, most prominently the shuttle mechanism which is believed to be the main cause of capacity decay and low Coulombic efficiency [147–149].

### 8.3.1 Graphene in Lithium-Sulfur Batteries Cathodes

The highest limitations for the technological application of sulfur cathodes are the electrical and ionic insulating nature of sulfur ( $5 \times 10^{-30} \text{ S cm}^{-1}$ ) [150] and the formation of lithium polysulfides during discharge, which reduce the capacity upon cycling (Figure 8.6) [151]. Several strategies, such as the incorporation of conductive additives (i.e., carbon or metals) and the use of organic electrolytes, have been developed to augment the electrical conductivity of the cathode. Nevertheless, the insulating character of sulfur and polysulfides, is not the only challenge in Li-S cells. Another big issue that must be

consider is related with the solubility of the long chain polysulfides intermediates ( $\text{Li}_2\text{S}_x$ ,  $2 < x < 8$ ) generated upon reduction by lithium in an organic electrolyte [152]. These intermediates can be involved in the sulfur shuttle mechanism whereby sulfur active mass is lost through irreversible redox reactions of polysulfides at both, the positive and negative electrode surfaces [153]. Furthermore, another common drawback for sulfur is its large volume expansion during lithiation ( $\sim 80\%$ ) which can result in a breakdown of the electrode. This shortcoming is usually addressed by using conductive additives able to accommodate volume expansion and, at the same time, improve electrical conductivity [154]. Recently, some groups have tried to solve these problems incorporating conductive, porous and elastically buffer materials into the cathode. In this context, graphene appears as a very good candidate due to its high surface area [11], superior electronic conductivity [155] and high mechanical strength [156].

Graphene due to its high specific surface area can achieve a high sulfur loading; also, it has a superior electronic conductivity which can facilitate electron transport not only across the sulfur, but also in cathodes without the addition of any conducting filler. However, graphene is not the most effective matrix material to confine the polysulfides in cathodes during the discharge/charge processes, while reduced graphene oxide (RGO), with oxygen functional groups, has been used as an alternative to alleviate the shuttle problem [157], due the presence of functional groups in RGO that interact with the polysulfides. The different methodologies used

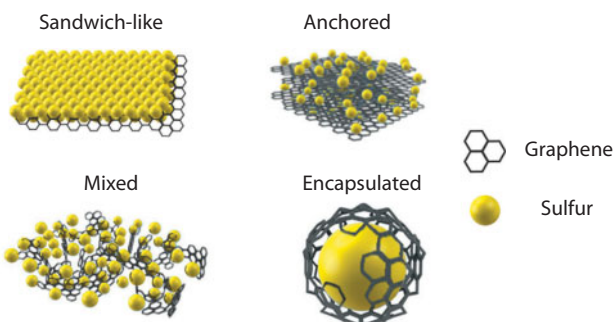


**Figure 8.7** Schematic of the different structures of graphene composite electrode materials. Sandwich-like model: Graphene is used as a template to generate active material/graphene sandwich structures. Anchored: electroactive nanoparticles are anchored to the graphene surface. Mixed: Graphene and active materials are synthesized separately and mixed mechanically during the electrode preparation. Encapsulated or wrapped: The active-material particles are wrapped or encapsulated by graphene single or multiple graphene sheets.

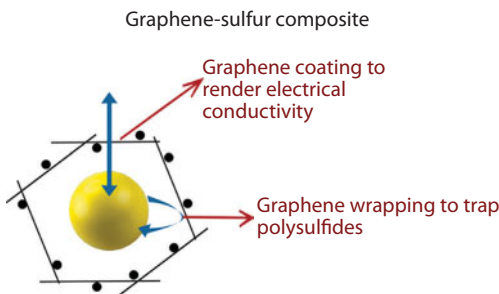


Figure 8.8 Scheme of the synthesized nanocomposite based on Wang *et al.*, [158].

to incorporate graphene or graphene oxide on cathodes for Li-S batteries were classified by Raccinchini *et al.*, [43] in four main groups: encapsulated or wrapped, mixed, anchored and sandwich like model, Figure 8.7. This section summarizes some designs of graphene based cathodes aimed to improve its conductivity and to achieve complete containment of sulfur and limit dissolution of polysulfides in the electrolyte.

One of the first reports of graphene as constituent of the cathode in Li-S batteries was published in 2011 using the encapsulation strategy. Wang *et al.*, [158] reported the synthesis of a graphene-sulfur composite material by encapsulating poly(ethylene glycol) (PEG) coated sub-micrometer sulfur particles with mildly oxidized graphene oxide sheets decorated by carbon black nanoparticles. They highlighted the importance of PEG and graphene coating layers to accommodate the volume expansion of the coated sulfur particles during discharge, trapping soluble polysulfide intermediates, and rendering the sulfur particles electrically conducting, Figure 8.8. The resulting graphene sulfur composite showed high and stable specific capacities up to  $\sim 600$  mAh g $^{-1}$  over more than 100 cycles. More recently, Liu *et al.*, [159] reported the use of a graphene-enveloped sulfur composite material as cathode for Li-S batteries. The composite was prepared via the redox reaction between sodium polysulfide and graphene oxide without any extra reducing agents. Across the analysis of SEM images, XRD data and FT-IR results, they confirmed the perfect encapsulation of sulfur spheres into a graphene shell. The as prepared material was mixed with carbon black, and PVDF in a ratio of 8:1:1 wt.% and spread on pure aluminum foil to use as cathode. This is the standard procedure to elaborate sulfur cathodes and the one which is used in all further examples, unless mention otherwise. The cells presented an initial capacity of 827 mAh g $^{-1}$  at 0.2 C with a remnant specific capacity of 388 mAh g $^{-1}$  after 100 cycles. The authors associated the fast capacity fading with the

presence of uncovered sulfur particles, which reinforce the necessity of a complete coverage of sulfur particles by graphene in order to isolate them from the electrolyte.

Taking advantage of the role of graphene wrapped sulfur particles, Nazar and Evers [160] reported a very interesting work about graphene-sulfur composites with a sulfur loading as high as 87 wt.%. The samples were prepared by combining a mixture of graphene oxide and soluble polysulfide. Half batteries prepared with this active material as electrodes achieved a specific discharged capacity of  $575 \text{ mAh g}^{-1}$  after 30 cycles (at  $1.4 \text{ A g}^{-1}$ ), and a coulombic efficiency of 93%. Nazar and Evers emphasized the importance on using partially oxidized graphene not only as an electrical conduit for insulating sulfur, but also as a barrier to retard polysulfide dissolution. The improvement on the electrochemical performance is associated with two opposite characteristics of graphene. On one hand, its highly graphitic and conductive character and, in the other hand, the slightly hydrophilic properties due to the presence of oxo-groups on the carbon surface, which aid in polysulfide binding.

In a later study, Sun *et al.*, [150] developed a similar strategy based on a one-pot wet chemical method to encapsulate sulfur into the interlayer space of graphene sheets. They varied systematically the sulfur content in the composite, from 20.9 wt.% to 72.5 wt.%, and founded a dependence of the cycling stability and rate capability on it. Electrodes prepared with high-sulfur content evidenced the formation of S particles of about hundreds of nanometers in size, decreasing the amount of electroactive sulfur for cycling. Contrary, in the low-sulfur content samples a greater percentage of the sulfur is gradually dissolved in the electrolyte giving 63.6 wt.% as best sulfur loading. These allowed an uniform accommodation of sulfur on the graphene sheets, preserving the high conductivity of the composite ( $1.30 \text{ S cm}^{-1}$ ) and enhancing the transportation of lithium ions and electrolyte. In this way, they demonstrated the importance of intimate relationship between the sulfur content and the graphene utilization, responsible of the electrochemical performances of the composite electrode. Batteries prepared with the composite containing 63.6 wt.% of S delivered a reversible capacity as high as  $804 \text{ mAh g}^{-1}$  after 80 cycles at a current density of  $312 \text{ mA g}^{-1}$ . Similar results were founded by Jin *et al.*, [161], who used a graphene-sulfur paper with a 67 wt.% of sulfur loading to prepare an electrode with a high conductivity of  $4.71 \text{ S cm}^{-1}$  and a reversible discharge capacity of  $600 \text{ mAh g}^{-1}$  after 100 cycles.

Considering the importance of sulfur content and the presence of oxygen functions on graphene, in order to achieve high specific energy densities and to successfully restrain lithium polysulfides, respectively,

different studies have been performed. Yoo *et al.*, [162] reported, in 2016, the synthesis and utilization of a composite based on sulfur and reduce graphene oxide (RGO). The nanostructured material consisted in one-dimensional tubular structure spirally wrapped graphene sheet embedded with well-dispersed nano-sized sulfur. The as-prepared composite, with a sulfur loading of 76 wt.%, exhibited an initial capacity of  $1295 \text{ mAh g}^{-1}$  and reversible capacity of  $744 \text{ mAh g}^{-1}$  after 100 cycles at 0.2 C. Contrarily, using unscrolled GO sheet, the capacity fed continuously to  $510 \text{ mAh g}^{-1}$  after 100 cycles, due to the irreversible loss of sulfur by the dissolution of polysulfides. The experimental results indicated that the scrolled graphene provides reversible reaction sites and acts as an effective physical barrier for polysulfides, increasing the cycling properties in the Li-S batteries. However, the enhanced performance of the composite used as cathode, seems to be a result not only from the RGO's scrolled structures, but also from the nano-sized and well-dispersed sulfur. The synergic combination of both materials allows the effective access of sulfur to  $\text{Li}^+$  in electrolyte as well as a very efficiently electron conduction through graphene.

As was mentioned before, another strategy to improve overall electrochemical performance of Li-S batteries is to use graphene as host for more complex structures, such as sandwich-type ones. Xie *et. al* [163], for example, published an interesting study using 5–10 layers graphene as part of a 3D hierarchical sandwich-type graphene sheet-sulfur/carbon composite. They founded that the great flexibility of graphene allows obtaining a good interconnected graphene network which facilitates the fast electron/ion transference, improving the electrical conductivity of the cathode. Electrodes prepared in this way presented an initial discharge capacity of  $1171 \text{ mAh g}^{-1}$  and a capacity retention of 48% after 120 cycles. Tian *et al.*, [164] used a graphene-mesoporous carbon/sulfur composites (G-MPC/S) prepared by melt-infiltration of sulfur as cathode of Li-S batteries. The combination of graphene and mesoporous carbon enhanced long cycling performance of the cathode indicating that graphene sheets can create more microporous structure and improve the cyclability by efficiently suppressing the shuttling effect and accommodating sulfur volume expansion-contraction during the discharge-charge processes. In addition, an outstanding coulombic efficiency (nearly 100 %) of the G-MPC/S composite was obtained during 200 cycles. These excellent cycling stability and electrochemical reversibility proved that the diffusion and dissolution of soluble polysulfides is more effectively restrained by the combination of graphene and mesoporous carbon. Following a different strategy, Cao *et al.*, [165] proposed the use of a functionalized graphene sheet-sulfur (FGSS) nanocomposite as cathode material for Li-S batteries. The nanocomposite

was synthesized by mixing carbon disulfide with functionalized graphene and treating the mixture thermally under nitrogen gas. They found that the FGSS nanocomposite electrode delivered a reasonably high initial discharge capacity of  $950 \text{ mAh g}^{-1}$ , which is comparable favorably with other carbon based materials. This graphene based composite, conceptually provided a new strategy for designing electrodes in energy storage application and opened the horizons to several studies conducted to determine the best combination of graphene and sulfur for battery purposes.

Another possible structure containing graphene and sulfur is the mixed one, Figure 8.7, which take place when both materials are mechanically mixed during electrode preparation. Wang *et al.*, [166] reported an interesting and innovative work in which they were able to increase the sulfur content in the whole battery by making a binder free and free standing electrode. This technique had a few advantages; as there was no need of the aluminum foil then, the total mass of the cathode was decreased, and, the traditional electrode making process was avoided. It is worth mentioning the fact that the conductivity was increased by dispensing with the PVDF binder. This approach consisted in using a sulfur/graphene paper material which served directly as an electrode for the Li-S battery. This means that the paper acted as both conducting agent and current collector. The RGO paper was synthesized via a facile freeze drying route followed by low-temperature heat treatment, in this way a final S content of 63 wt.% was achieved. It also has many characteristics that improved electrochemical performance when was used as an electrode of Li-S battery. First, polysulfides are trapped in the many adhesion points and physical barriers present in the S-RGO paper therefore reducing the shuttle effect. Second, the flexible nature can relieve mechanical stress generated during cycling due to volumetric expansion of sulfur, and hence improve the stability of the electrode. Consequently, the initial specific discharge capacity was of  $1072 \text{ mAh g}^{-1}$  and the coulombic efficiency of 99%; after 200 cycles, the capacity decreased to  $889 \text{ mAh g}^{-1}$ , with still nearly a 100% efficiency. These facts showed that the S-RGO paper had a stable cycling performance and might be considered for the next generation Li-S batteries.

There is another structure that has been studied in sulfur-graphene based cathodes which consisted in anchored electroactive nanoparticles to the graphene surface. Ma *et al.*, [167] fabricated a ultrafine nano sulfur particles anchored on *in-situ* exfoliated graphene by dielectric barrier discharge plasma. The material presented a 69.2% of sulfur content anchored to a defect graphene skeleton. High reversible capacities of  $753.6 \text{ mAh g}^{-1}$  and stable coulombic efficiencies close to 100% were obtained at 0.5 C. The great electrochemical performance was associated with the presence

of: (i) ultrafine nano-sulfur which shortens the transport distance of ions and electrons mitigating also the volume expansion; (ii) the little oxygen-doping in graphene skeleton which could facilitate the capturing capacity towards lithium polysulfides promoting not only the electron and ion conductivity of inner sulfur, but also alleviates volume expansion.

Even the already demonstrated advantages of incorporating reduce graphene oxide in cathodes, there is another drawback to overcome. In some cases, RGO is not able to achieve high enough electrical conductivity, and it is necessary to include a 15–20 wt.% of carbon black additives in the cathode which leads to a lower S loading in the final cathode. Following this line, there was a big progress by the utilization of nitrogen doped graphene to achieve Li-S cells with high capacity and long cycle life. Qiu *et al.*, [168] have prepared a cathode using only N-doped graphene (NG) wrapping S and PVDF, without carbon black additives. The cathodes, containing 60 wt.% of S respect to the total weight, have exhibited high specific capacity (978 mAh g<sup>-1</sup>), an excellent rate performance up to 5 C and an ultra-long cycle life up to 2000 cycles at 2 C, with a decay rate of 0.028% per cycle. The authors related this outstanding performance of the cells to (a) the presence of highly conductive NG sheets with a large surface wrapping S nanoparticles which resulted in the significant improvement of electronic conductivity of the overall S cathode; (b) the curvature and wrinkles created on the NG sheets during the synthetic process which brought out many cavities facilitating not only the electrolyte access throughout the structure, but also buffering the volume expansion/contraction of S during discharge/charge cycles; and (c) the favorable ionic attraction between the N functional groups of NG sheets and the intermediate higher-order lithium polysulfides helping on trapping these species, affecting also their redeposition process upon discharge/charge.

The work done by Qiu *et al.*, [168] have inspired other authors to incorporate NG as cathode material. Lu *et al.*, [169], for example, proposed a facile strategy by using N-doped graphene as an immobilizer to stabilize sulfur and its discharge products. The method that they followed for making the NG consisted in putting GO under NH<sub>3</sub> gas flow at 400 °C. The resulting NG was mixed with sulfur via a melt-diffusion method, with a final sulfur content of 70 wt.%. This composite delivered a capacity of 880 mAh g<sup>-1</sup> at 0.3 A g<sup>-1</sup> with an excellent Coulombic efficiency and high cycle stability. Also exhibited a good capacity retention meaning a 0.05% capacity decay per cycle up to 300 cycles. These results led to insights about the roles played by the doped N atom in graphene network on the electrochemical reaction, the incorporated nitrogen dopants were found to have a strong binding effect on the

lithium polysulfides improving electrochemical stability and promoting fast electrochemical reaction kinetics. This N-doped graphene cathode exhibited a high specific capacity, fast reaction dynamics, good rate performance, and stable cycling performance. Song *et al.*, [170] reported a highly crumpled nitrogen-doped graphene sheet as sulfur host for Li-S batteries. They demonstrated that the large surface area of the NG enables not only a greater sulfur loading during the preparation of the composite, but also can enhance the affinity and binding energy of the nonpolar carbon atoms with polar polysulfides, alleviating their dissolution towards the electrolyte and the consequent shuttle effect. Cells using an 80 wt.% of synthesized nitrogen-doped graphene sheet and 10 wt.% of carbon additives, showed a specific capacity of 1227 mAh g<sup>-1</sup> and a long-cycle life of 200 cycles. More recently, Liu *et al.*, [171] proposed the use N-doped reduced graphene oxide as sulfur host for cathodes. The structure combined the presence of nanopores; which provide more space for sulfur, that can accommodate volume expansion and improve accessibility to the electrolyte; with the presence of two types of nitrogen functional groups: pyridinic and pyrrolic N, which suppress the lithium polysulfide shuttling. The obtained composite delivered high reversible discharge capacity of 1110 mAh g<sup>-1</sup> at 1 C rate, with a Coulombic efficiency of 100% and a retention capacity of 70.5% after 110 cycles.

In summary a great number of studies have showed that the use of graphene, reduce graphene oxide or nitrogen doped graphene are good as a buffer materials into the cathode and as potential solutions to the problems associated to the cathode in Li-S batteries. Each one of these materials have achieved, by large, to overcome the drawbacks of sulfur cathodes by increasing ionic and electronic conductivity, reducing the shuttle effect, improving cycling performance and accommodating volume expansion. Despite the fact that high capacities and cycle stability were delivered, the fabricated cathodes are not suitable for commercial purposes, since higher performance are needed. In conclusion graphene, RGO and NG have proved themselves as candidates to be used as substrates of Li-S batteries cathodes, but still there is work to be done in the many lines of research that they have opened.

### 8.3.2 Graphene in Lithium-Sulfur Batteries Separators

It is well known that there are practical problems that need to be overcome to achieve competitive Li-S batteries to be applicable in electric vehicles. These are, the low electronic and ionic conductivity of solid S

and secondary products that are formed while it is in operation like polysulfides (PS), large volume changes, and the shuttle effect [140, 172–174]. One strategy to avoid this last issue is to modify separators in order to trap, block or repel polysulfides.

The separators are one essential part in the batteries with the fundamental role of preventing the internal short-circuit while allowing the diffusion of ions through it [175, 176]. Polymeric porous separators (polypropylene-polyethylene) are efficient in achieving this in lithium ion cells. However, for the special case of the lithium-sulfur cell, separators do not repel or impede, but even allow high polysulfide mobility to the anode due their high porosity [177]. An approach to prevent polysulfide diffusion and/or migration to the lithium anode is a selective barrier for polysulfides.

In this sense, separators are perfect platforms for modification, which can introduce novel cell configuration for Li-S batteries. An ideal Li-S batteries separator should [178, 179]:

- suppress polysulfide diffusion through electrostatic repulsion or steric hindrance.
- be an electrically insulating layer to separate anode and cathode.
- allow an efficient diffusion of lithium ions ( $\text{Li}^+$ ).
- have robust mechanical properties.
- be easy to integrate as a functional layer.

Nevertheless it is important to notice that this extra barrier could retard  $\text{Li}^+$  diffusion and also, enhance the internal resistance of the cell. Hence it is important to achieve the best compromise to balancing the high permeability and ionic conduction necessities in a separator and the specific impermeability for PS.

Next, different strategies used to stop the diffusion of polysulfides by modifying the separator will be described. Various functional layers, including polymers, carbons, oxides and composites of them, have been applied to modify the separators in order to achieve a better battery performance.

Different types of carbon-based polysulfide barriers have been recently tested as an additional interlayer between the polyolefin separator and sulfur cathode. This has shown to be a promising approach owing to its simple fabrication process, low cost and especially the highly improved rate capability and cycling stability. These approaches include the use of: carbon super P [180], microporous carbon paper [181], multiwall carbon

nanotubes (MWCNTs) [182], graphene [183], graphene oxide [184] and reduced graphene oxide [185], to enhance the cycling performances of Li-S batteries [186]. There are also reports using these carbonaceous materials combined with polymers [179, 185, 187–189] or different nanostructures [190–192], such as modified carbon nanotubes or nanostructured oxides [193], that improve the cell performance.

The use of graphene oxide (GO) as coating material in Li-S barriers have been investigated, since their rich functional groups in the carbon framework could significantly reduce the shuttle mechanism by hindering the polysulfide migration due to their interaction with the oxygen functional groups while providing a high permselectivity for the lithium ions [194]. Huang *et al.*, [195] obtained by filtration an ultrathin GO membrane on the celgard attaining a low capacity decay rate of only 0.23% per cycle. Figure 8.9 illustrates how the negatively charged GO membrane keeps the polysulfide species on the cathode side. Zhang *et al.*, [196] coated a separator with a mixture of GO and oxidized-carbon nanotubes (O-CNT) improving the specific capacities of Li-S cell to 750 mAh g<sup>-1</sup> at 1 C after 100 cycles. The interconnected nanoscale channels provided by O-CNT add up to the binding forces induced by functional groups in GO restrict the polysulfide movement but allowing Li ions diffusion to the anode. The mass ratio of the coating is much less than for other modifications, which guarantees a high capacity of the whole battery. In another work Jiang

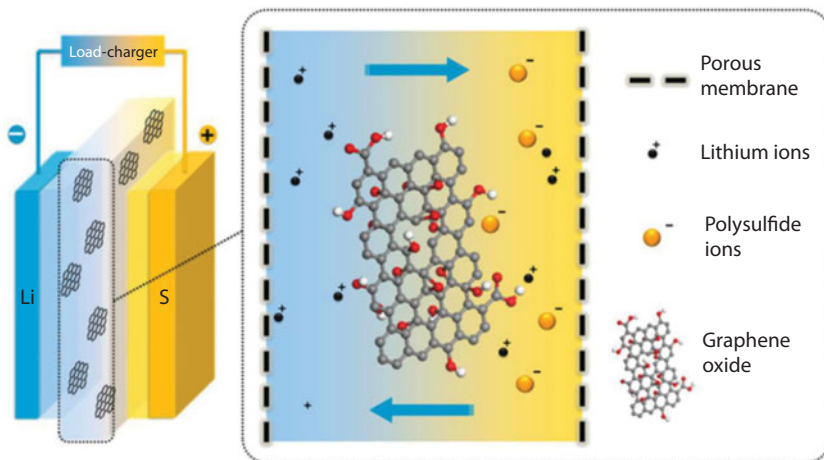


**Figure 8.9** A scheme of a GO membrane inside a Li-S battery. The GO membrane is sandwiched between the cathode and anode electrodes. GO may efficiently prevent the shuttle of polysulfides through the membrane. Reproduced with permission from Ref [195]. Copyright 2015, American Chemical Society.

*et al.*, [186] used a high-flux GO coated separator with high stability, maintaining the three-dimensional porous structure even after long cycles and the resultant Li-S cell delivered an impressive capacity retention with a high S utilization because of this high-ordered structure.

Reduced graphene oxide, which has been widely used in S cathodes, is another promising material for coating the separators since it is a two dimensional (2D) structure material with preminent electrical conductivity and high surface to volume ratio. Depending upon the degree of reduction, RGO can be obtained with various oxygen contents and surface areas [197]. Zhu *et al.*, [198] explored the relationship between the reduction degree of RGO and PS retardation. Their results indicate that RGO with higher reduction degree is more effective in retarding the PS shuttling. The cells with high-reduction degree RGO-coated separator maintained a capacity of  $733 \text{ mAhg}^{-1}$  after 100 cycles and delivered a high capacity of  $519 \text{ mAhg}^{-1}$  at 2C, which were 42% and 92% higher than those of cells with low-reduction degree RGO-coated separator. Wang *et al.*, [199] used a RGO based film sandwiched between a sulfur cathode and the separator acting as a shuttle inhibitor to the sulfur and polysulfides. This freestanding graphene film was derived through vacuum filtration of GO dispersion followed by thermal treatment. It needs to mention that RGO sheets are tightly stacked, which difficult the ions diffusion by the electrolyte. Thus they introduced carbon black (CB) nanoparticles to enlarge the gaps between neighboring graphene layers. The lithium-sulfur cell delivered an initial discharge capacity of  $1260 \text{ mAh g}^{-1}$  and the capacity remained at  $895 \text{ mAh g}^{-1}$  after 100 cycles. A three-dimensional (3D) reduced graphene oxide/activated carbon film (RGO/AC), synthesized by a simple hydro-thermal method and mechanical pressing by Li *et al.*, [200] showed that the introduction of activated carbons, in this case, effectively mitigates the restack of graphene while also serving as anchors points from which the graphene nanosheets are pinned around. The RGO/AC acting as a functional interlayer showed an initial discharge capacity of  $1078 \text{ mAh g}^{-1}$  and a reversible capacity of  $655 \text{ mAh g}^{-1}$  after 100 cycles. This inhibited the shuttle effect during the charge/discharge, and also promoted a higher utilization of active materials thought the recycling of entrapped active materials improving the capacity and the coulombic efficiency of Li-S cells.

Considering the possibilities of obtaining different graphene derivative from RGO [201] Vizintin *et al.* [202] reported the synthesis of fluorinated reduced graphene oxide (F-RGO) by a direct fluorination of RGO. F-RGO has been used as an interlayer additive supported by a glass fiber separator in lithium-sulfur (Li-S). Electrochemical cycling of Li-S batteries confirmed the beneficial role of F-RGO separators, with a more pronounced effect observed

for high degrees of fluorination. Also a better reversibility and better capacity retention was achieved upon cycling and the authors analyzed to the relative amounts of  $Li_2S$  and polysulfides found in the separator interlayer by XPS analysis that prove the efficiency of this kind of separator in blocking diffusion/migration of polysulfides from the positive electrode to the metallic lithium anode.

Kim *et al.*, [203] prepared ultrathin nitrogen and sulfur co-doped graphene (NSG) nanosheets layer and deposited them on a polyethylene (PE) separator for lithium-sulfur battery. The results showed that the surface of the separator has an homogeneous morphology with uniform surface coverage by NSG nanosheets, which were strongly adhered to the surface of the PE separator without any agglomeration. NSG provided mechanical reinforcement preserving the mechanical integrity of the separator and effectively suppressing the dendrite growth and maintaining a uniform ionic flux to the metal surface. The battery with an NSG-coated separator was remarkably improved when comparing to a cell with an uncoated polyethylene separator.

Other strategies to modify the separator consisted in using graphene and GO with polymers or different combinations adding other compounds like carbonaceous structures, polymers among others. Below are listed some of the most promising results using these techniques.

In this sense, Ou *et al.*, [204] synthesized a monolayer of graphene by chemical vapor deposition (CVD) as an interlayer to coat a piece of Celgard and resulted in an improvement of the specific capacity. Then they sealed the bigger holes of the modified separator with *in situ* polymerized nylon-66 via an interfacial polymerization reaction, obtaining nylon-66-sealed graphene/polypropylene separator which enhance the electrochemical performance notably by letting lithium to cross-over the modified separator but not the polysulfides. They also carried out molecular dynamics simulations to understand the impact of the size and structure of graphene pores in reducing the shuttle effect founding that there is a critical diameter of the pores in order to prevent lithium polysulfides to freely go through the graphene.

Similarly, Du *et al.*, [205] developed a two-layer CVD-formed graphene supported on the polypropylene separator (2G-PP) resulting in a flexible and robust separator [205]. In this system the cell showed an enhanced specific capacity up to 1500 cycles and a good reversibility. The Li–S battery assembled with 2G-PP delivered initial specific discharge capacities 11% higher than the analogous battery assembled with bare-PP at 0.1 and 0.5 C. Also, the discharge plateaus of the cells assembled with the graphene modified separator were longer. These results indicate that the resulting cells with 2G-PP have enhanced specific capacity, cycle performance, and

rate capability and suppressed self-discharge compared to the bare-PP analogues. This is a considerable improvement over the cell containing bare-PP.

Following a similar strategy, a dual functional separator composed by graphene/Celgard/ $\text{Al}_2\text{O}_3$  was studied. The modified separator not only enhances  $\text{Li}^+$  and electron transport thanks to conductive layer of graphene, but also prevents undesirable contact between the cathode and lithium dendrites formed on the anode thanks to the  $\text{Al}_2\text{O}_3$  coating. As result, the electrode, with sulfur loading of about  $4.0 \text{ mg cm}^{-2}$ , delivers a discharge capacity as high as  $1375 \text{ mAh g}^{-1}$  at  $0.1 \text{ C}$  rate, a superior rate capability up to  $5 \text{ C}$ , and cycling stability for 200 cycles at  $1 \text{ C}$  [191].

The combination of GO with polymers is another well-known strategy to minimized the shuttle effect. Several polymers have been used to this purpose which can principally be classified as linear, branched and permselective. Using a linear polymer, Zhu *et al.*, [206] have built a membrane separator based on a highly porous polyacrylonitrile and graphene oxide (PAN/GO). Cells prepared with this membrane, presented an enhancement not only in the cyclability, but also in the rate capability respect to the analogous prepared without GO. This improvement is attributed to the synergic combination of the physical and chemical barrier provided by PAN with GO. The highly porous structure and good wettability of PAN/GO nanofibers allow the diffusion of  $\text{Li}^+$  while avoiding the polysulfide diffusion. Measurement of ionic conductivity results in values of  $0.6$ ;  $1.00$  and  $1.36 \text{ mS cm}^{-1}$  for Celgard, Celgard with PAN and PAN/GO, respectively, confirming the higher diffusion rate of  $\text{Li}^+$  when PAN/GO is used [206]. Comparing the three different separators analyzed, it was observed that the discharge capacity of the Li-S cell was higher when more electronegative groups were present in the separator. These results are associated not only with the enhancement of the  $\text{Li}^+$  conductivity, but also with the relatively increasing binding energies between the  $-\text{C}\equiv\text{N}$  of PAN and polysulfides. Additionally, they observed that after 100 cycles, the cell with PAN/GO separator still delivered a high capacity of  $597 \text{ mAh g}^{-1}$  which is 38% higher than that of the cell with PP separator. These modified separators block effectively the PS transport and further enhance the utilization of the active material.

Another commonly used polymer used to reduce the shuttle mechanism is Nafion. Zhuang *et al.*, [207] reported a ternary-layered separator based on PP/GO/Nafion. An ultrathin layer of GO was deposited, blocking the macropores of PP matrix. After that, a ion selective Nafion membrane was attached to the PP/GO to suppress the cross-over of sulfur-containing species. This modification allowed a better sulfur utilization, improving

the efficiency and cyclability of the battery due to the suppression of polysulfides and the protection of the lithium anode.

In general terms, when using modified separators, there is always the compromise between the thickness of the layer and its ability to block, trap or diminish the transport of polysulfides. In this case, functionalized graphene is the one that is useful for preventing the shuttle mechanism in lithium sulfur batteries, and it is important to achieve a good compromise between the fluxes of lithium ions against the polysulfide transfer.

### 8.3.3 Graphene for Lithium Anode Protection in Lithium-Sulfur Batteries

Aside from the problems associated with the sulfur cathode, the highly reactive Li metal anode challenges the successful implementation of Li-S batteries. Although lithium metal has an extremely high specific capacity ( $\sim 3860 \text{ mAh g}^{-1}$ ) [208] and lower negative redox potential ( $-3.04 \text{ V}$  versus standard hydrogen electrode), the high reactivity in conventional electrolytes, low cycling efficiency and dendritic growth during cycling represents formidable challenges for future usage. Different from the classical layered graphite anode in LIBs, Li metal is a “hostless” anode. The working mechanism for Li anode is  $\text{Li}^+$  plating/stripping from the anode instead of intercalation/de-intercalation in graphite anode during charge/discharge process. During the repeated charge-discharge cycling, the continuous uneven deposition and stripping of lithium induce uncontrollable growth of lithium dendrites, which not only breaks solid electrolyte interfacial film and leads to the generation of “dead Li” with low Coulombic efficiency, but also induces safety hazards (like internal short circuit, combustion/explosion of full cells) since it can penetrate through the polymer separator and form micro-short circuits between the positive and negative electrodes, causing the serious safety issues including fire and even explosions [209, 210]. At the same time, as soluble lithium polysulfide species can easily migrate from the cathode through the porous separator and react with the lithium-metal anode, the study and protection of lithium anode is of tremendous importance. Moreover, the electrolyte continued to be consumed due to the high reactivity of fresh lithium, so a reduced cycle life is obtained by Li-S battery. Confronting with these damages of lithium anodes are critical to be addressed for the achievement of high-performance lithium-sulfur batteries. The Li metal anode protection can be achieved by efficiently regulating the diffusion and distribution behavior of Li ions and electrons.

Graphene has also been implemented to overcome these issues. Its two dimensional structure and flexibility has dropped the attentions to use it as an artificial electrode-electrolyte separator, avoiding the direct contact causing electrolyte consumption and mechanically suppressing the dendrite formation. Zhang *et al.*, [211] presented a facile automatic spreading method to coat metallic lithium surface with graphene oxide. This covering manages to diminish dendrite formation displaying a better stability upon cycling. Bobnar *et al.*, [212] used fluorinated reduced graphene oxide to cover lithium surface. They showed an enhanced electrochemical performance testing a full cell battery system with two different types of cathodes. Although this is relatively new research topic, it has taken great attentions due to the potential use of metallic lithium anodes in future Li-S and Li-Air batteries. The further exploration on rational integration of these strategies is highly expected to afford more fundamental understanding and engineering applications to practical Li metal batteries.

## 8.4 Conclusions and Outlooks

Due to graphene's intrinsic properties, such as high electrical conductivity, chemical surface versatility, high specific surface area and mechanical strength, its application on rechargeable lithium batteries is being extensively studied. In this chapter, we aimed to summarize the different applications of graphene over all the parts of lithium-based batteries: cathode, anode and separator. We also analysed the benefits of its use in lithium-ion and lithium-sulfur batteries.

Regarding lithium-ion batteries, graphene has been used as active material, additive, support or as part of a composite for anodic active materials. Pristine mono and bi-layer graphene cannot be efficiently used as LIB anode active materials due to its high delithiation voltage, the poor energy-storage efficiency, and the massive irreversible capacity associated with the SEI formation. In fact, the only material that could compete with state-of-art graphite anodes is multilayer graphene structures, but in this case the main disadvantage is related to these materials' low density outputting low volumetric capacities. Nonetheless, several studies have demonstrated that the use of graphene as additive helps preventing the agglomeration of active material nano/microparticles used in anodes, improving the electron conductivity,  $\text{Li}^+$  mobility and enhancing the mechanical stability of the whole electrode. In the case

of alloying based anodes, such as silicon and tin, it also helps buffering the changes in the volume suffered by these materials during charge and discharge cycles.

As for cathodes, graphene has been used as an additive during the synthesis of the cathodic active materials following the same strategies as for anode materials. Even though its presence enhances the storage capacity of the battery; an optimal concentration of it should be used. It was demonstrated that the addition of an excess of graphene is a setback for ionic conduction, which is one of the cornerstones in the additive's state-of-art for developing high power density electrodes. The best results were achieved when graphene is used in combination with other carbon sources, such as carbon black which mitigates graphene's blocking nature of  $\text{Li}^+$  diffusion. It is important to determine the best proportion of graphene/metal oxide/extra-carbon to achieve a synergistic effect between all components thus improving the electrochemical behaviour in each cathode material.

In the case of lithium-sulfur batteries, graphene could help not only to diminish the impact of sulfur's insulating nature, but also to buffer the volume changes. Furthermore, if graphene is functionalized it could prevent the occurrence of the shuttle mechanism, by the interaction of the functional groups with lithium polysulfides as pointed out recently in several reports. All these features improve the usage of the active material and enhance the overall performance of the battery. For separators, graphene and its derivatives are widely used to impede or reduce the migration of soluble polysulfides, reducing in this way the shuttle mechanism and improving the electrochemical behaviour. Recently, graphene derivatives were also used to protect lithium metal anodes preventing the Li dendrites growth and its consequent degradation.

In conclusion, graphene and its derivatives have proved to have interesting applications for its use in rechargeable lithium batteries although we should lower the expectations that these materials have generated in scientific community. Generally speaking, for graphene utilization on an industrial scale it is necessary to find a strategic compromise to reduce production costs, simplifying the synthetic routes and improving the reproducibility of the obtained graphene. Large-scale, reproducible and functional groups density and nature-controlled synthesis routes are still needed taking into account the impact of these latter factors in the final properties of graphene-derived materials. Its promising reported applications open the door for using it in the near future as additive in lithium batteries, although more systematic studies are need. Also, and as a general rule for batteries research field, scientific community needs to be more

thorough as to which metrics use for reporting electrochemical and long-term battery performance.

## References

1. Hannan, M.A., Hoque, M.M., Hussain, A., Yusof, Y., Ker, P.J., *et al.*, State-of-the-art and energy management system of lithium-ion batteries in electric vehicle applications: issues and recommendations. *IEEE Access*, 6, 19362–19378, 2018.
2. Jaiswal, A., Lithium-ion battery based renewable energy solution for off-grid electricity: A techno-economic analysis. *Renew Sustain Energy Rev*, 2017.
3. Hannan, M.A., Hoque, M.M., Hussain, A., Yusof, Y., Ker, P.J., *et al.*, State-of-the-art and energy management system of lithium-Ion batteries in electric vehicle applications: issues and recommendations. *IEEE Access*, 6, 19362–19378, 2018.
4. Yoshino, A., The birth of the lithium-ion battery. *Angew Chemie - Int Ed*, 2012.
5. Owen, J.R., Rechargeable lithium batteries. *Chem. Soc. Rev.*, 1997.
6. Batteries, H.O.F., Library, D.E., Companies, T.M., *Handbook of batteries. Cell*, 2004.
7. Kim, J.K., Choi, J.W., Chauhan, G.S., Ahn, J.H., Hwang, G.C., Choi, J.B., *et al.*, Enhancement of electrochemical performance of lithium iron phosphate by controlled sol–gel synthesis. *Electrochim. Acta*, 53(28), 8258–8264, 2008.
8. Winter, M., Brodd, R.J., What are batteries, fuel cells, and supercapacitors? *Chem. Rev.*, 104(10), 4245–4270, 2004.
9. Peled, E., Menkin, S., Review—SEI: Past, Present and Future. *J. Electrochem. Soc.*, 2017.
10. Team MEV, A guide to understanding battery specifications. *Current*, 1–3, 2008.
11. Kay, G.F., American association for the advancement of science. *Science*, 39(80), 398–405, 1914.
12. Randviir, E.P., Brownson, D.A.C., Banks, C.E., A decade of graphene research: production, applications and outlook. *Materials Today*, 17(9), 426–432, 2014.
13. Chen, K., Wang, Q., Niu, Z., Chen, J., Graphene-based materials for flexible energy storage devices. *J. Energy Chem.*, 2017.
14. Dong, Y., Wu, Z.S., Ren, W., Cheng, H.-M., Bao, X., *et al.*, Graphene: a promising 2D material for electrochemical energy storage. *Science Bulletin*, 62(10), 724–740, 2017.
15. WM, W., Zhang, C.S., Bin, Y.S., Controllable synthesis of sandwich-like graphene-supported structures for energy storage and conversion. *Xinxing Tan Cailiao/New Carbon Mater*, 2017.

16. Li, Y., Yang, J., Song, J., Nano energy system model and nanoscale effect of graphene battery in renewable energy electric vehicle. *Renewable and Sustainable Energy Reviews*, 69, 652–663, 2017.
17. Cai, X., Lai, L., Shen, Z., Lin, J., Graphene and graphene-based composites as Li-ion battery electrode materials and their application in full cells. *J Mater Chem A Mater Chem A*, 2017.
18. Wen, L., Li, F., Luo, H.Z., Cheng, H.M., Graphene for flexible lithium-ion batteries: development and prospects. . *Nanocarbons Adv Energy Storage*, 2015.
19. Zhu, J., Duan, R., Zhang, S., Jiang, N., Zhang, Y., Zhu, J., *et al.*, The application of graphene in lithium ion battery electrode materials. *Springerplus*, 3, 585, 2014.
20. Li, X., Zhi, L., Graphene hybridization for energy storage applications. *Chem. Soc. Rev.*, 47(9), 3189–3216, 2018.
21. Placke, T., Kloepsch, R., Dühnen, S., Winter, M., Lithium ion, lithium metal, and alternative rechargeable battery technologies: the odyssey for high energy density. *J. Solid State Electrochem.*, 21(7), 1939–1964, 2017.
22. Andre, D., Kim, S.-J., Lamp, P., Lux, S.F., Maglia, F., Paschos, O., *et al.*, Future generations of cathode materials: an automotive industry perspective. *J. Mater. Chem. A*, 3(13), 6709–6732, 2015.
23. Van Noorden, R., The rechargeable revolution: A better battery. *Nature*, 507(7490), 26–28, 2014.
24. Dahn, J.R., Zheng, T., Liu, Y., Xue, J.S., Mechanisms for lithium insertion in carbonaceous materials. *Science*, 270(80), 590–593, 1995.
25. Sato, K., Noguchi, M., Demachi, A., Oki, N., Endo, M., A mechanism of lithium storage in disordered carbons. *Science*, 264(80), 556–558, 1994.
26. Yoo, E., Kim, J., Hosono, E., Zhou, H.S., Kudo, T., Honma, I., *et al.*, Large reversible Li storage of graphene nanosheet families for use in rechargeable lithium ion batteries. *Nano Lett.*, 8(8), 2277–2282, 2008.
27. Pan, D., Wang, S., Zhao, B., Wu, M., Zhang, H., Wang, Y., *et al.*, Li Storage Properties of Disordered Graphene Nanosheets. *Chem. Mater.*, 21(14), 3136–3142, 2009.
28. Wang, D., Kou, R., Choi, D., Yang, Z., Nie, Z., Li, J., *et al.*, Ternary self-assembly of ordered metal oxide-graphene nanocomposites for electrochemical energy storage. *ACS Nano*, 4(3), 1587–1595, 2010.
29. Du, Z., Yin, X., Zhang, M., Hao, Q., Wang, Y., Wang, T., *et al.*, *In situ* synthesis of SnO<sub>2</sub>/graphene nanocomposite and their application as anode material for lithium ion battery. *Mater. Lett.*, 64(19), 2076–2079, 2010.
30. Wu, Z.S., Ren, W., Xu, L., Li, F., Cheng, H.M., Doped graphene sheets as anode materials with superhigh rate and large capacity for lithium ion batteries. *ACS Nano*, 5(7), 5463–5471, 2011.
31. Li, X., Geng, D., Zhang, Y., Meng, X., Li, R., Sun, X., *et al.*, Superior cycle stability of nitrogen-doped graphene nanosheets as anodes for lithium ion batteries. *Electrochem. commun.*, 13(8), 822–825, 2011.

32. Wang, H.-guo., Wang, Y., Li, Y., Wan, Y., Duan, Q., *et al.*, Exceptional electrochemical performance of nitrogen-doped porous carbon for lithium storage. *Carbon N Y*, 82, 116–123, 2015.
33. Liu, X., Wu, Y., Yang, Z., Pan, F., Zhong, X., Wang, J., *et al.*, Nitrogen-doped 3D macroporous graphene frameworks as anode for high performance lithium-ion batteries. *J. Power Sources*, 293, 799–805, 2015.
34. Yan, Y., Yin, Y.X., Xin, S., Guo, Y.G., Wan, L.J., Ionothermal synthesis of sulfur-doped porous carbons hybridized with graphene as superior anode materials for lithium-ion batteries. *Chem. Commun. (Camb.)*, 48(86), 10663–10665, 2012.
35. Ai, W., Xie, L., Du, Z., Zeng, Z., Liu, J., Zhang, H., *et al.*, A novel graphene-polysulfide anode material for high-performance lithium-ion batteries. *Sci. Rep.*, 3, 2341, 2013.
36. Zhang, C., Mahmood, N., Yin, H., Liu, F., Hou, Y., Chenzhen, Z., Nasir, M., Han, Y., Synthesis of phosphorus-doped graphene and its multifunctional applications for oxygen reduction reaction and lithium ion batteries. *Adv. Mater. Weinheim.*, 25(35), 4932–4937, 2013.
37. Wang, Z.L., Xu, D., Wang, H.G., Wu, Z., Zhang, X.B., *In situ* fabrication of porous graphene electrodes for high-performance energy storage. *ACS Nano*, 7(3), 2422–2430, 2013.
38. Ma, X., Ning, G., Sun, Y., Pu, Y., Gao, J., *et al.*, High capacity Li storage in sulfur and nitrogen dual-doped graphene networks. *Carbon N Y*, 79, 310–320, 2014.
39. David, L., Singh, G., Reduced graphene oxide paper electrode: opposing effect of thermal annealing on Li and Na cyclability. *J. Phys. Chem. C*, 118(49), 28401–28408, 2014.
40. Kang, Y.R., Li, Y.L., Hou, F., Wen, Y.Y., Su, D., Fabrication of electric papers of graphene nanosheet shelled cellulose fibres by dispersion and infiltration as flexible electrodes for energy storage. *Nanoscale*, 4(10), 3248–3253, 2012.
41. Compton, O.C., Jain, B., Dikin, D.A., Abouimrane, A., Amine, K., Nguyen, S.T., *et al.*, Chemically active reduced graphene oxide with tunable C/O ratios. *ACS Nano*, 5(6), 4380–4391, 2011.
42. Rinaldo, R., Alberto, V., Di, W., Stefano, P., Critical insight into the relentless progression toward graphene andgraphene-containing materials for lithium-ion battery anodes. *Adv. Mater. Weinheim.*, 29, 1603421, 2017.
43. Raccichini, R., Varzi, A., Passerini, S., Scrosati, B., The role of graphene for electrochemical energy storage. *Nat. Mater.*, 14(3), 271–279, 2015.
44. Kokai, F., Sorin, R., Chigusa, H., Hanai, K., Koshio, A., Ishihara, M., *et al.*, Ultrasonication fabrication of high quality multilayer graphene flakes and their characterization as anodes for lithium ion batteries. *Diam. Relat. Mater.*, 29, 63–68, 2012.
45. Mukherjee, R., Thomas, A.V., Krishnamurthy, A., Koratkar, N., Photothermally reduced graphene as high-power anodes for lithium-ion batteries. *ACS Nano*, 6(9), 7867–7878, 2012.

46. Xiang, H.F., Li, Z.D., Xie, K., Jiang, J.Z., Chen, J.J., Lian, P.C., *et al.*, Graphene sheets as anode materials for Li-ion batteries: preparation, structure, electrochemical properties and mechanism for lithium storage. *RSC Adv.*, 2(17), 6792–6799, 2012.
47. Chen, C.M., Zhang, Q., Huang, J.Q., Zhang, W., Zhao, X.C., Huang, C.H., *et al.*, Chemically derived graphene–metal oxide hybrids as electrodes for electrochemical energy storage: pre-graphenization or post-graphenization? *J. Mater. Chem.*, 22(28), 13947–13955, 2012.
48. Robledo, C.B., Otero, M., Luque, G., Cámaras, O., Barraco, D., Rojas, M.I., *et al.*, First-principles studies of lithium storage in reduced graphite oxide. *Electrochim. Acta*, 140, 232–237, 2014.
49. Robledo, C.B., Thomas, J.E., Luque, G., Leiva, E.P.M., Cámaras, O., Barraco, D., *et al.*, An experimental and theoretical approach on the effect of presence of oxygen in milled graphite as lithium storage material. *Electrochim. Acta*, 140, 160–167, 2014.
50. Yao, F., Güneş, F., Ta, H.Q., Lee, S.M., Chae, S.J., Sheem, K.Y., *et al.*, Diffusion mechanism of lithium ion through basal plane of layered graphene. *J. Am. Chem. Soc.*, 134(20), 8646–8654, 2012.
51. Liu, Y., Artyukhov, V.I., Liu, M., Harutyunyan, A.R., Yakobson, B.I., Feasibility of lithium storage on graphene and its derivatives. *J. Phys. Chem. Lett.*, 4(10), 1737–1742, 2013.
52. Pollak, E., Geng, B., Jeon, K.J., Lucas, I.T., Richardson, T.J., Wang, F., *et al.*, The interaction of Li<sup>+</sup> with single-layer and few-layer graphene. *Nano Lett.*, 10(9), 3386–3388, 2010.
53. Liu, J.Y., Li, X.X., Huang, J.R., Li, J.J., Zhou, P., Liu, J.H., *et al.*, Three-dimensional graphene-based nanocomposites for high energy density Li-ion batteries. *J. Mater. Chem. A*, 5(13), 5977–5994, 2017.
54. Wytse, H.A., Yejung, C., Kwang-dong, S., *et al.*, Recent progress in porous graphene and reduced graphene oxide-based nanomaterials for electrochemical energy storagedevices. *Adv. Mater. Interfaces*, 5, 1701212, 2017.
55. XL, W., Guo, Y.G., Wan, L.J., Rational design of anode materials based on group iva elements (Si, Ge, and Sn) for lithium-ion batteries. *Chem - An Asian J.*, 8, 1948–1958, 2013.
56. Yang, X., Wen, Z., Xu, X., Lin, B., Lin, Z., High-performance silicon/carbon/graphite composites as anode materials for Lithium Ion Batteries. *J. Electrochem. Soc.*, 153(7), A1341–1344, 2006.
57. Nitta, N., Wu, F., Lee, J.T., Yushin, G., Li-ion battery materials: present and future. *Materials Today*, 18(5), 252–264, 2015.
58. Wang, J.-Z., Zhong, C., Chou, S.-L., Liu, H.-K., Flexible free-standing graphene-silicon composite film for lithium-ion batteries. *Electrochim. commun.*, 12(11), 1467–1470, 2010.
59. Zhao, X., Hayner, C.M., Kung, M.C., Kung, H.H., In-Plane Vacancy-Enabled High-Power Si-Graphene Composite Electrode for Lithium-Ion Batteries. *Adv. Energy Mater.*, 1(6), 1079–1084, 2011.

60. Luo, J., Zhao, X., Wu, J., Jang, H.D., Kung, H.H., Huang, J., *et al.*, Crumpled graphene-encapsulated Si nanoparticles for lithium ion battery anodes. *J. Phys. Chem. Lett.*, 3(13), 1824–1829, 2012.
61. Zhou, M., Li, X., Wang, B., Zhang, Y., Ning, J., Xiao, Z., *et al.*, High-Performance Silicon Battery Anodes Enabled by Engineering Graphene Assemblies. *Nano Lett.*, 15(9), 6222–6228, 2015.
62. Ashuri, M., He, Q., Shaw, L.L., Silicon as a potential anode material for Li-ion batteries: where size, geometry and structure matter. *Nanoscale*, 8(1), 74–103, 2016.
63. Kun, F., Matthew, L., Wenwen, L., *et al.*, Silicon-Based Anodes for Lithium-Ion Batteries: From Fundamentals to Practical Applications. *Small*, 14, 1702737, 2018.
64. Franco. Gonzalez, A., Yang, N.-H., Liu, R.-S., Silicon Anode Design for Lithium-Ion Batteries: Progress and Perspectives. *J. Phys. Chem. C*, 121(50), 27775–27787, 2017.
65. Wei, L., Xinqi, C., Yuan, X., *et al.*, Surface and Interface Engineering of Silicon-Based Anode Materials for Lithium-Ion Batteries. *Adv. Energy Mater.*, 7, 1701083, 2017.
66. Lee, J.K., Smith, K.B., Hayner, C.M., Kung, H.H., Silicon nanoparticles-graphene paper composites for Li ion battery anodes. *Chem. Commun. (Camb.)*, 46(12), 2025, 2010.
67. Zhou, X., Yin, Y.-X., Wan, L.-J., Guo, Y.-G., Self-assembled nanocomposite of silicon nanoparticles encapsulated in graphene through electrostatic attraction for lithium-ion batteries. *Adv. Energy Mater.*, 2(9), 1086–1090, 2012.
68. Zhou, X., Cao, A.-M., Wan, L.-J., Guo, Y.-G., Spin-coated silicon nanoparticle/graphene electrode as a binder-free anode for high-performance lithium-ion batteries. *Nano Res.*, 5(12), 845–853, 2012.
69. Wang, B., Li, X., Zhang, X., Luo, B., Zhang, Y., Zhi, L., Bin, W., Xianglong, L., Xianfeng, Z., *et al.*, Contact-engineered and void-involved silicon/carbon nanohybrids as lithium-ion-battery anodes. *Adv. Mater. Weinheim.*, 25(26), 3560–3565, 2013.
70. Hassan, F.M., Batmaz, R., Li, J., Wang, X., Xiao, X., Yu, A., *et al.*, Evidence of covalent synergy in silicon-sulfur-graphene yielding highly efficient and long-life lithium-ion batteries. *Nat. Commun.*, 6, 8597, 2015.
71. Urquiza, M.L., Otero, M., Luque, G.L., Barraco, D., Leiva, E.P.M., *et al.*, First-Principles studies of silicon underpotential deposition on defective graphene and its relevance for lithium-ion battery materials. *Electrochim. Acta*, 208, 92–101, 2016.
72. Zhao, Y., Li, X., Yan, B., Li, D., Lawes, S., Sun, X., *et al.*, Significant impact of 2D graphene nanosheets on large volume change tin-based anodes in lithium-ion batteries: A review. *J. Power Sources*, 274, 869–884, 2015.
73. Liu, L., Xie, F., Lyu, J., Zhao, T., Li, T., Choi, B.G., *et al.*, Tin-based anode materials with well-designed architectures for next-generation lithium-ion batteries. *J. Power Sources*, 321, 11–35, 2016.

74. Qin, J., He, C., Zhao, N., Wang, Z., Shi, C., Liu, E.Z., *et al.*, Graphene networks anchored with sn@graphene as lithium ion battery anode. *ACS Nano*, 8(2), 1728–1738, 2014.
75. Chen, S., Wang, Y., Ahn, H., Wang, G., Microwave hydrothermal synthesis of high performance tin–graphene nanocomposites for lithium ion batteries. *J. Power Sources*, 216, 22–27, 2012.
76. Kim, C., Noh, M., Choi, M., Cho, J., Park, B., *et al.*, Critical Size of a Nano SnO<sub>2</sub> Electrode for Li-Secondary Battery. *Chem. Mater.*, 17(12), 3297–3301, 2005.
77. Zou, Y., Wang, Y., Sn@CNT nanostructures rooted in graphene with high and fast Li-storage capacities. *ACS Nano*, 5(10), 8108–8114, 2011.
78. Deng, Y., Fang, C., Chen, G., The developments of SnO<sub>2</sub>/graphene nanocomposites as anode materials for high performance lithium ion batteries: A review. *J. Power Sources*, 304, 81–101, 2016.
79. Jahel, A., Ghimbeu, C.M., Monconduit, L., Vix-Guterl, C., Confined Ultrasmall SnO<sub>2</sub> Particles in Micro/Mesoporous Carbon as an Extremely Long Cycle-Life Anode Material for Li-Ion Batteries. *Adv. Energy Mater.*, 4(11), 1400025–1400027, 2014.
80. Xu, G., Han, P., Dong, S., Liu, H., Cui, G., Chen, L., Li<sub>4</sub>Ti<sub>5</sub>O<sub>12</sub>-based energy conversion and storage systems: Status and prospects. *Coord. Chem. Rev.*, 343, 139–184, 2017.
81. Zhao, B., Ran, R., Liu, M., Shao, Z., A comprehensive review of Li<sub>4</sub>Ti<sub>5</sub>O<sub>12</sub>-based electrodes for lithium-ion batteries: The latest advancements and future perspectives. *Materials Science and Engineering: R: Reports*, 98, 1–71, 2015.
82. Chauque, S., Oliva, F.Y., Visintin, A., Barraco, D., Leiva, E.P.M., Cámar, O.R., *et al.*, Lithium titanate as anode material for lithium ion batteries: Synthesis, post-treatment and its electrochemical response. *Journal of Electroanalytical Chemistry*, 799, 142–155, 2017.
83. Wang, Y.Q., Gu, L., Guo, Y.G., Li, H., He, X.Q., Tsukimoto, S., *et al.*, Rutile-TiO<sub>2</sub> nanocoating for a high-rate Li<sub>4</sub>Ti<sub>5</sub>O<sub>12</sub> anode of a lithium-ion battery. *J. Am. Chem. Soc.*, 134(18), 7874–7879, 2012.
84. Jie, W., Hailei, Z., Zhaolin, L., *et al.*, Revealing Rate Limitations in Nanocrystalline Li<sub>4</sub>Ti<sub>5</sub>O<sub>12</sub> Anodes for High-Power Lithium Ion Batteries. *Adv. Mater. Interfaces*, 3, 1600003, 2016.
85. T-F, Y., Xie, Y., Wu, Q., *et al.*, High rate cycling performance of lanthanum-modified Li<sub>4</sub>Ti<sub>5</sub>O<sub>12</sub> anode materials for lithium-ion batteries. *J. Power Sources*, 214, 220–226, 2012.
86. Sun, Y.-K., Jung, D.-J., Lee, Y.S., Nahm, K.S., Synthesis and electrochemical characterization of spinel Li[Li(1-x)/3Cr<sub>x</sub>Ti(5-2x)/3]O<sub>4</sub> anode materials. *J. Power Sources*, 125(2), 242–245, 2004.
87. Binitha, G., Siva, R.K., Shantikumar, N., Dhamodaran, S., Impact of Carbon Nanostructures as Additives with Spinel Li<sub>4</sub>Ti<sub>5</sub>O<sub>12</sub>/LiMn<sub>2</sub>O<sub>4</sub> Electrodes for Lithium Ion Battery Technology. *ChemistrySelect*, 2, 9772–9776, 2017.

88. Yoon, S.-B., Kim, H.-K., Roh, K.C., Kim, K.-B., Electrochemical Kinetics Investigation of  $\text{Li}_{4/3}\text{Ti}_{5/6}\text{O}_{12}$ /Reduced Graphene Oxide Nanocomposite Using Voltammetric Charge Analysis. *J. Electrochem. Soc.*, 162(4), A667–A673, 2015.
89. Ding, Z., Zhao, L., Suo, L., Jiao, Y., Meng, S., Hu, Y.S., *et al.*, Towards understanding the effects of carbon and nitrogen-doped carbon coating on the electrochemical performance of  $\text{Li}_{4}\text{Ti}_{5}\text{O}_{12}$  in lithium ion batteries: a combined experimental and theoretical study. *Phys. Chem. Chem. Phys.*, 13(33), 15127–15133, 2011.
90. Kim, J., Kim, J.Y., Pham-Cong, D., Jeong, S.Y., Chang, J., Choi, J.H., *et al.*, Individually carbon-coated and electrostatic-force-derived graphene-oxide-wrapped lithium titanium oxide nanofibers as anode material for lithium-ion batteries. *Electrochim. Acta*, 199, 35–44, 2016.
91. Ge, H., Hao, T., Osgood, H., Zhang, B., Chen, L., Cui, L., *et al.*, Advanced Mesoporous Spinel  $\text{Li}_{4}\text{Ti}_{5}\text{O}_{12}/\text{rGO}$  Composites with Increased Surface Lithium Storage Capability for High-Power Lithium-Ion Batteries. *ACS Appl. Mater. Interfaces*, 8(14), 9162–9169, 2016.
92. Meng, T., Yi, F., Cheng, H., Hao, J., Shu, D., Zhao, S., *et al.*, Preparation of Lithium Titanate/Reduced Graphene Oxide Composites with Three-Dimensional "Fishnet-Like" Conductive Structure via a Gas-Foaming Method for High-Rate Lithium-Ion Batteries. *ACS Appl. Mater. Interfaces*, 9(49), 42883–42892, 2017.
93. Kucinskis, G., Bajars, G., Kleperis, J., Graphene in lithium ion battery cathode materials: A review. *J. Power Sources*, 2013.
94. Levasseur, S., Ménétrier, M., Delmas, C., On the dual effect of Mg doping in  $\text{LiCoO}_2$  and  $\text{Li}_{1+\delta}\text{CoO}_2$ : Structural, electronic properties, and  $^{7}\text{Li}$  MAS NMR studies. *Chem. Mater.*, 2002.
95. Dokko, K., Mohamedi, M., Fujita, Y., *et al.*, Kinetic Characterization of Single Particles of  $\text{LiCoO}_{2}$  by AC Impedance and Potential Step Methods. *J. Electrochem. Soc.*, 2001.
96. Cao, F., Prakash, J., A comparative electrochemical study of  $\text{LiMn}_2\text{O}_4$  spinel thin-film and porous laminate. *Electrochim. Acta*, 47(10), 1607–1613, 2002.
97. Marzec, *et al.*, Conduction mechanism in operating a  $\text{LiMn}_2\text{O}_4$  cathode. *Solid State Ionic.*, 146(3-4), 225–237, 2002.
98. Prosini, P., Lisi, M., Zane, D., Pasquali, M., Determination of the chemical diffusion coefficient of lithium in  $\text{LiFePO}_4$ . *Solid State Ionic.*, 148(1-2), 45–51, 2002.
99. Shi, S., Liu, L., Ouyang, C., Enhancement of electronic conductivity of  $\text{LiFePO}_4$  by Cr doping and its identification by first-principles calculations. *Phys. Rev. B - Condens. Matter Mater. Phys.*, 2003.
100. Pan, A., Choi, D., Zhang, J.-G., Liang, S., Cao, G., Nie, Z., *et al.*, High-rate cathodes based on  $\text{Li}_3\text{V}_2(\text{PO}_4)_3$  nanobelts prepared via surfactant-assisted fabrication. *J. Power Sources*, 196(7), 3646–3649, 2011.

101. Calderón, C.A., Thomas, J.E., Lener, G., Barraco, D.E., Visintin, A., *et al.*, Electrochemical comparison of LiFePO<sub>4</sub> synthesized by a solid-state method using either microwave heating or a tube furnace. *J. Appl. Electrochem.*, 47(10), 1179–1188, 2017.
102. FY, S., YB, H., Li, B., *et al.*, Could graphene construct an effective conducting network in a high-power lithium ion battery? *Nano Energy*, 1, 429–439, 2012.
103. Mo, R., Lei, Z., Rooney, D., Sun, K., Facile synthesis of nanocrystalline LiFePO<sub>4</sub>/graphene composite as cathode material for high power lithium ion batteries. *Electrochim. Acta*, 130, 594–599, 2014.
104. Lim, J., Gim, J., Song, J., Nguyen, D.T., Kim, S., Jo, J., *et al.*, Direct formation of LiFePO<sub>4</sub>/graphene composite via microwave-assisted polyol process. *J. Power Sources*, 304, 354–359, 2016.
105. Du, Y., Tang, Y., Chang, C., Enhanced electrochemical performance from 3DG/LiFePO<sub>4</sub>/G sandwich cathode material. *Journal of Physics and Chemistry of Solids*, 107, 36–41, 2017.
106. Gupta, H., Kataria, S., Balo, L., Singh, V.K., Singh, S.K., Tripathi, A.K., *et al.*, Electrochemical study of Ionic Liquid based polymer electrolyte with graphene oxide coated LiFePO<sub>4</sub> cathode for Li battery. *Solid State Ionic.*, 320, 186–192, 2018.
107. Wei, X., Guan, Y., Zheng, X., Zhu, Q., Shen, J., Qiao, N., *et al.*, Improvement on high rate performance of LiFePO<sub>4</sub> cathodes using graphene as a conductive agent. *Appl. Surf. Sci.*, 440, 748–754, 2018.
108. Guler, A., Duman, S.O., Nalci, D., *et al.*, Graphene assisted template based LiMn<sub>2</sub>O<sub>4</sub> flexible cathode electrodes. *Int J Energy Res*, 2018.
109. Luo, D., Fang, S., Yang, L., Hirano, S.I., Preparation of Layered-Spinel Microsphere/Reduced Graphene Oxide Cathode Materials for Ultrafast Charge-Discharge Lithium-Ion Batteries. *ChemSusChem*, 10(24), 4845–4850, 2017.
110. Tang, R., Yun, Q., Lv, W., He, Y.-B., You, C., Su, F., *et al.*, How a very trace amount of graphene additive works for constructing an efficient conductive network in LiCoO<sub>2</sub>-based lithium-ion batteries. *Carbon N Y*, 103, 356–362, 2016.
111. Rui, X., Sim, D., Wong, K., Zhu, J., Liu, W., Xu, C., *et al.*, Li<sub>3</sub>V<sub>2</sub>(PO<sub>4</sub>)<sub>3</sub> nanocrystals embedded in a nanoporous carbon matrix supported on reduced graphene oxide sheets: Binder-free and high rate cathode material for lithium-ion batteries. *J. Power Sources*, 214, 171–177, 2012.
112. Jiang, Y., Xu, W., Chen, D., Jiao, Z., Zhang, H., Ma, Q., *et al.*, Graphene modified Li<sub>3</sub>V<sub>2</sub>(PO<sub>4</sub>)<sub>3</sub> as a high-performance cathode material for lithium ion batteries. *Electrochim. Acta*, 85, 377–383, 2012.
113. Liu, H., Yang, G., Zhang, X., Gao, P., Wang, L., Fang, J., *et al.*, Kinetics of conventional carbon coated-Li<sub>3</sub>V<sub>2</sub>(PO<sub>4</sub>)<sub>3</sub> and nanocomposite Li<sub>3</sub>V<sub>2</sub>(PO<sub>4</sub>)<sub>3</sub>/graphene as cathode materials for lithium ion batteries. *J. Mater. Chem.*, 22(22), 11039, 2012.

114. Zhu, J., Yang, R., Wu, K., Synthesis of Li<sub>3</sub>V<sub>2</sub>(PO<sub>4</sub>)<sub>3</sub>/reduced graphene oxide cathode material with high-rate capability. *Ionics*, 19(4), 577–580, 2013.
115. Liu, H., Gao, P., Fang, J., Yang, G., Li<sub>3</sub>V<sub>2</sub>(PO<sub>4</sub>)<sub>3</sub>/graphene nanocomposites as cathode material for lithium ion batteries. *Chem. Commun.*, 47(32), 9110–9112, 2011.
116. Lian, P., Zhu, X., Liang, S., Li, Z., Yang, W., Wang, H., *et al.*, Large reversible capacity of high quality graphene sheets as an anode material for lithium-ion batteries. *Electrochim. Acta*, 55(12), 3909–3914, 2010.
117. Xu, H., Chang, J., Sun, J., Gao, L., Graphene-encapsulated LiFePO<sub>4</sub> nanoparticles with high electrochemical performance for lithium ion batteries. *Mater. Lett.*, 83, 27–30, 2012.
118. Zhu, X., Hu, J., Wu, W., Zeng, W., Dai, H., Du, Y., *et al.*, LiFePO<sub>4</sub>/reduced graphene oxide hybrid cathode for lithium ion battery with outstanding rate performance. *J. Mater. Chem. A*, 2(21), 7812–7818, 2014.
119. Wang, X., Feng, Z., Huang, J., Deng, W., Li, X., Zhang, H., *et al.*, Graphene-decorated carbon-coated LiFePO<sub>4</sub> nanospheres as a high-performance cathode material for lithium-ion batteries. *Carbon N Y*, 127, 149–157, 2018.
120. Wang, H., Yang, Y., Liang, Y., *et al.*, LiMn<sub>1-x</sub>Fe<sub>x</sub>PO<sub>4</sub> nanorods grown on graphene sheets for ultrahigh-rate-performance lithium ion batteries. *Angew Chemie - Int.* 50. pp. 7364–7368, 2011.
121. Luo, X.D., Yin, Y.Z., Yuan, M., Zeng, W., Lin, G., Huang, B., *et al.*, High performance composites of spinel LiMn<sub>2</sub>O<sub>4</sub>/3DG for lithium ion batteries. *RSC Adv.*, 8(2), 877–884, 2018.
122. Yang, M., Ren, M., Zhu, W., Liu, W., Zhu, C., *et al.*, Li<sub>3</sub>V<sub>2</sub>(PO<sub>4</sub>)<sub>3</sub>/graphene nanocomposites with superior cycling performance as cathode materials for lithium ion batteries. *Electrochim. Acta*, 182, 1046–1052, 2015.
123. Wang, L., Wang, H., Liu, Z., Xiao, C., Dong, S., Han, P., *et al.*, A facile method of preparing mixed conducting LiFePO<sub>4</sub>/graphene composites for lithium-ion batteries. *Solid State Ionic.*, 181(37–38), 1685–1689, 2010.
124. Ding, Y., Jiang, Y., Xu, F., Yin, J., Ren, H., Zhuo, Q., *et al.*, Preparation of nano-structured LiFePO<sub>4</sub>/graphene composites by co-precipitation method. *Electrochim. Commun.*, 12(1), 10–13, 2010.
125. Su, C., Bu, X., Xu, L., Liu, J., Zhang, C., *et al.*, A novel LiFePO<sub>4</sub>/graphene/carbon composite as a performance-improved cathode material for lithium-ion batteries. *Electrochim. Acta*, 64, 190–195, 2012.
126. Xu, H., Chang, J., Sun, J., Gao, L., Graphene-encapsulated LiFePO<sub>4</sub> nanoparticles with high electrochemical performance for lithium ion batteries. *Mater. Lett.*, 83, 27–30, 2012.
127. Wang, X., Feng, Z., Huang, J., Deng, W., Li, X., Zhang, H., *et al.*, Graphene-decorated carbon-coated LiFePO<sub>4</sub> nanospheres as a high-performance cathode material for lithium-ion batteries. *Carbon N Y*, 127, 149–157, 2018.
128. Drezen, T., Kwon, N.-H., Bowen, P., Teerlinck, I., Isono, M., Exnar, I., *et al.*, Effect of particle size on LiMnPO<sub>4</sub> cathodes. *J. Power Sources*, 174(2), 949–953, 2007.

129. Martha, S.K., Markovsky, B., Grinblat, J., *et al.*, LiMnPO<sub>4</sub> as an Advanced Cathode Material for Rechargeable Lithium Batteries. *J. Electrochem. Soc.*, 2009.
130. Bakenov, Z., Taniguchi, I., Physical and electrochemical properties of LiMnPO<sub>4</sub>/C composite cathode prepared with different conductive carbons. *J. Power Sources*, 2010.
131. Choi, D., Wang, D., Bae, I.-T., Xiao, J., Nie, Z., Wang, W., *et al.*, LiMnPO<sub>4</sub> Nanoplate Grown via Solid-State Reaction in Molten Hydrocarbon for Li-Ion Battery Cathode. *Nano Lett.*, 10(8), 2799–2805, 2010.
132. Kang, B., Ceder, G., Electrochemical Performance of LiMnPO<sub>4</sub> synthesized with Off-Stoichiometry. *J. Electrochem. Soc.*, 157(7), A808, 2010.
133. Tang, M., Carter, W.C., Chiang, Y.-M., Electrochemically Driven Phase Transitions in Insertion Electrodes for Lithium-Ion Batteries: Examples in Lithium Metal Phosphate Olivines. *Annu. Rev. Mater. Res.*, 2010.
134. F-Y, S., You, C., Y-B, H., *et al.*, Flexible and planar graphene conductive additives for lithium-ion batteries. *J. Mater. Chem.*, 20, 9644, 2010.
135. Dominko, R., Gaberscek, M., Drofenik, J., *et al.*, The role of carbon black distribution in cathodes for Li ion batteries. *J. Power Sources*, 2003.
136. Dominko, R., Gaberšček, M., Drofenik, J., Bele, M., Jamnik, J., *et al.*, Influence of carbon black distribution on performance of oxide cathodes for Li ion batteries. *Electrochim. Acta*, 48(24), 3709–3716, 2003.
137. Murray, H.C., Al, E., Noag, N., *et al.*, United States Patent Office, 1962.
138. Zhang, X., Xie, H., Kim, C.-S., Zaghib, K., Mauger, A., Julien, C.M., *et al.*, Advances in lithium–sulfur batteries. *Materials Science and Engineering: R: Reports*, 121, 1–29, 2017.
139. Gröger, O., Gasteiger, H.A., Suchsland, J.-P., Review—Electromobility: Batteries or Fuel Cells? *J. Electrochem. Soc.*, 162(14), A2605–A2622, 2015.
140. Yin, Y.X., Xin, S., Guo, Y.G., Wan, L.J., Lithium-sulfur batteries: Electrochemistry, materials, and prospects. *Angew Chemie - Int Ed*, 2013.
141. Hagen, M., Hanselmann, D., Ahlbrecht, K., Lithium-Sulfur Cells: The Gap between the State-of-the-Art and the Requirements for High Energy Battery Cells. *Adv. Energy Mater.*, 2015.
142. Nitta, N., Wu, F., Lee, J.T., Yushin, G., Li-ion battery materials: present and future. *Materials Today*, 18(5), 252–264, 2015.
143. Cleaver, T., Kovacik, P., Marinescu, M., Zhang, T., Offer, G., *et al.*, Perspective—Commercializing Lithium Sulfur Batteries: Are We Doing the Right Research? *J. Electrochem. Soc.*, 165(1), A6029–A6033, 2018.
144. Lang, J., Qi, L., Luo, Y., Wu, H., High performance lithium metal anode: Progress and prospects. *Energy Storage Materials*, 7, 115–129, 2017.
145. Kumar, R., Liu, J., Hwang, J.-Y., Sun, Y.-K., Recent research trends in Li–S batteries. *J. Mater. Chem. A*, 6(25), 11582–11605, 2018.
146. Zhang, X., Xie, H., Kim, C.-S., Zaghib, K., Mauger, A., Julien, C.M., *et al.*, Advances in lithium–sulfur batteries. *Materials Science and Engineering: R: Reports*, 121, 1–29, 2017.

147. Cheon, S.-E., Choi, S.-S., Han, J.-S., Choi, Y.-S., Jung, B.-H., Lim, H.S., *et al.*, Capacity Fading Mechanisms on Cycling a High-Capacity Secondary Sulfur Cathode. *J. Electrochem. Soc.*, 151(12), A2067, 2004.
148. Xu, R., Belharouak, I., Zhang, X., *et al.*, Insight into Sulfur Reactions in Li – S Batteries. *ACS Appl. Mater. Interfaces*, 2014.
149. Yan, J., Liu X, L.B., Capacity fade analysis of sulfur cathodes in lithium– sulfur batteries. *Adv. Sci.*, 2016.
150. Sun, H., Xu, G., Xu, Y., *et al.*, A Composite Material of Uniformly Dispersed Sulfur on Reduced Graphene Oxide : Aqueous One-Pot Synthesis. *Characterization and Excellent Performance as the Cathode in Rechargeable Lithium – Sulfur Batteries*, 3, 676–684, 2012.
151. Wild, M., O'Neill, L., Zhang, T., Purkayastha, R., Minton, G., Marinescu, M., *et al.*, Lithium sulfur batteries, a mechanistic review. *Energy Environ. Sci.*, 8(12), 3477–3494, 2015.
152. Manthiram, A., Fu, Y., Su, Y.-S., Challenges and Prospects of Lithium–Sulfur Batteries. *Acc. Chem. Res.*, 46(5), 1125–1134, 2013.
153. Diao, Y., Xie, K., Xiong, S., Hong, X., Shuttle phenomenon – The irreversible oxidation mechanism of sulfur active material in Li–S battery. *J. Power Sources*, 235, 181–186, 2013.
154. Seh, Z.W., Li, W., Cha, J.J., *et al.*, Sulphur–TiO<sub>2</sub> yolk–shell nanoarchitecture with internal void space for long-cycle lithium–sulphur batteries *Zhi. Nat. Commun.*, 4, 1–6, 2012.
155. Geim, A.K., Novoselov, K.S., The rise of graphene. *Nat. Mater.*, 6(3), 183–191, 2007.
156. Ovid'ko, I.A., Mechanical properties of graphene. *Rev Adv Mater Sci*, 1–11, 2013.
157. Yang, X., Zhang, L., Zhang, F., *et al.*, Sulfur-Infiltrated Graphene-Based Layered Porous Carbon Cathodes for. *ACS Nano*, 8, 5208–5215, 2014.
158. Wang, H., Yang, Y., Liang, Y., Robinson, J.T., Li, Y., Jackson, A., *et al.*, Graphene-wrapped sulfur particles as a rechargeable lithium-sulfur battery cathode material with high capacity and cycling stability. *Nano Lett.*, 11(7), 2644–2647, 2011.
159. Liu, F., Liang, J., Zhang, C., Yu, L., Zhao, J., Liu, C., *et al.*, Reduced graphene oxide encapsulated sulfur spheres for the lithium-sulfur battery cathode. *Results in Physics*, 7, 250–255, 2017.
160. Evers, S., Nazar, L.F., New Approaches for High Energy Density Lithium–Sulfur Battery Cathodes. *Acc. Chem. Res.*, 46(5), 1135–1143, 2013.
161. Jin, J., Wen, Z., Ma, G., Lu, Y., Cui, Y., Wu, M., *et al.*, Flexible self-supporting graphene–sulfur paper for lithium sulfur batteries. *RSC Adv.*, 3(8), 2558–2560, 2013.
162. Yoo, S., Lee, J., Kim, J.M., Seong, C.-Y., Seong, K.-dong., Piao, Y., Min, J., *et al.*, Well-dispersed sulfur wrapped in reduced graphene oxide nanoscroll as cathode material for lithium–sulfur battery. *Journal of Electroanalytical Chemistry*, 780, 19–25, 2016.

163. Xie, J., Yang, J., Zhou, X., Zou, Y., Tang, J., Wang, S., *et al.*, Preparation of three-dimensional hybrid nanostructure-encapsulated sulfur cathode for high-rate lithium sulfur batteries. *J. Power Sources*, 253, 55–63, 2014.
164. Tian, T., Li, B., Zhu, M., *et al.*, Sandwich-like graphene-mesoporous carbon as sulfur host for enhanced lithium – sulfur batteries Sandwich-like graphene-mesoporous carbon as sulfur host for enhanced lithium – sulfur batteries. *Mater. Res. Express*, 4, 105017, 2017.
165. Cao, Y., Li, X., Aksay, I.A., Lemmon, J., Nie, Z., Yang, Z., *et al.*, Sandwich-type functionalized graphene sheet-sulfur nanocomposite for rechargeable lithium batteries. *Phys. Chem. Chem. Phys.*, 13(17), 7660–7665, 2011.
166. Wang, C., Wang, X., Wang, Y., Chen, J., Zhou, H., Huang, Y., Macroporous free-standing nano-sulfur/reduced graphene oxide paper as stable cathode for lithium-sulfur battery. *Nano Energy*, 11, 678–686, 2015.
167. Ma, Z., Tao, L., Liu, D., Li, Z., Zhang, Y., Liu, Z., *et al.*, Ultrafine nano-sulfur particles anchored on *in situ* exfoliated graphene for lithium–sulfur batteries. *J. Mater. Chem. A*, 5(19), 9412–9417, 2017.
168. Qiu, Y., Li, W., Zhao, W., *et al.*, High-Rate. *Ultralong Cycle-Life Lithium/Sulfur Batteries Enabled by Nitrogen-Doped Graphene*, 1–7, 2014.
169. Li, L., Zhou, G., Yin, L., Koratkar, N., Li, F., Cheng, H.-M., *et al.*, Stabilizing sulfur cathodes using nitrogen-doped graphene as a chemical immobilizer for Li S batteries. *Carbon N Y*, 108, 120–126, 2016.
170. Song, J., Yu, Z., Gordin, M.L., Wang, D., Advanced Sulfur Cathode Enabled by Highly Crumpled Nitrogen-Doped Graphene Sheets for High-Energy-Density Lithium–Sulfur Batteries. *Nano Lett.*, 16(2), 864–870, 2016.
171. Liu, S.-K., Hong, X.-B., Li, Y.-J., Xu, J., Zheng, C.-M., Xie, K., *et al.*, A nanoporous nitrogen-doped graphene for high performance lithium sulfur batteries. *Chin. Chem. Lett.*, 28(2), 412–416, 2017.
172. Deng, N., Kang, W., Liu, Y., Ju, J., Wu, D., Li, L., *et al.*, A review on separators for lithium sulfur battery: Progress and prospects. *J. Power Sources*, 331, 132–155, 2016.
173. Hagen, M., Hanselmann, D., Ahlbrecht, K., Maça, R., Gerber, D., Tübke, J., *et al.*, Lithium-Sulfur Cells: The Gap between the State-of-the-Art and the Requirements for High Energy Battery Cells. *Adv. Energy Mater.*, 5(16), 1401986, 2015.
174. Challenges, T., Challenges T *Li-S Batteries The Challenges, chemisrty, materials and futura perspectives*. Turkey, World Scientific Publishing Europe Ltd., Gebze Technical University.
175. Arora, P., Zhang, Zhengming (John), Zhang, Z., Battery Separators. *Chem. Rev.*, 104(10), 4419–4462, 2004.
176. Huang, J.-Q., Zhang, Q., Wei, F., Multi-functional separator/interlayer system for high-stable lithium-sulfur batteries: Progress and prospects. *Energy Storage Materials*, 1, 127–145, 2015.
177. Freitag, A., Stamm, M., Ionov, L., Separator for lithium-sulfur battery based on polymer blend membrane. *J. Power Sources*, 363, 384–391, 2017.

178. Deng, N., Kang, W., Liu, Y., *et al.*, A review on separators for lithium[sbnd]sulfur battery: Progress and prospects. *J. Power Sources*, 2016.
179. Liu, W., Jiang, J., Yang, K.R., Mi, Y., Kumaravadivel, P., Zhong, Y., *et al.*, Ultrathin dendrimer-graphene oxide composite film for stable cycling lithium-sulfur batteries. *Proc. Natl. Acad. Sci. USA.*, 114(14), 3578–3583, 2017.
180. Yao, H., Yan, K., Li, W., Zheng, G., Kong, D., Seh, Z.W., *et al.*, Improved lithium-sulfur batteries with a conductive coating on the separator to prevent the accumulation of inactive S-related species at the cathode-separator interface. *Energy Environ. Sci.*, 7(10), 3381–3390, 2014.
181. Su, Y. S., Manthiram, A., Lithium-sulphur batteries with a microporous carbon paper as a bifunctional interlayer. *Nat. Commun.*, 3(1), 2012.
182. Su, Y. S., Manthiram, A., A new approach to improve cycle performance of rechargeable lithium-sulfur batteries by inserting a free-standing MWCNT interlayer. *Chem. Commun.*, 48(70), 8817, 2012.
183. Li, F., Zhou, G., Pei, S., *et al.*, A graphene-pure-sulfur sandwich structure for ultrafast, long-life lithium-sulfur batteries. *Adv. Mater. Weinheim.*, 2014.
184. Huang, J.-Q., Xu, Z.-L., Abouali, S., Akbari Garakani, M., Kim, J.-K., *et al.*, Porous graphene oxide/carbon nanotube hybrid films as interlayer for lithium-sulfur batteries. *Carbon N Y*, 99, 624–632, 2016.
185. Lin, W., Chen, Y., Li, P., *et al.*, Enhanced Performance of Lithium Sulfur Battery with a Reduced Graphene Oxide Coating Separator. *J. Electrochem. Soc.*, 2015.
186. Jiang, Y., Chen, F., Gao, Y., Wang, Y., Wang, S., Gao, Q., *et al.*, Inhibiting the shuttle effect of Li-S battery with a graphene oxide coating separator: Performance improvement and mechanism study. *J. Power Sources*, 342, 929–938, 2017.
187. Yin, L., Dou, H., Wang, A., Xu, G., Nie, P., Chang, Z., *et al.*, A functional interlayer as a polysulfides blocking layer for high-performance lithium-sulfur batteries. *New J. Chem.*, 42(2), 1431–1436, 2018.
188. Zhuang, T., Huang, J., Peng, H., Rational Integration of Polypropylene / Graphene Oxide / Nafion as Ternary-Layered Separator to Retard the Shuttle of Polysulfides for Lithium – Sulfur Batteries381–389, 2016.
189. Ma, G., Huang, F., Wen, Z., Wang, Q., Hong, X., Jin, J., *et al.*, Enhanced performance of lithium sulfur batteries with conductive polymer modified separators. *J. Mater. Chem. A*, 4(43), 16968–16974, 2016.
190. Liu, M., Yang, Z., Sun, H., Lai, C., Zhao, X., Peng, H., *et al.*, A hybrid carbon aerogel with both aligned and interconnected pores as interlayer for high-performance lithium-sulfur batteries. *Nano Res.*, 9(12), 3735–3746, 2016.
191. Hwang, J.-Y., Kim, H.M., Shin, S., Sun, Y.-K., Designing a High-Performance Lithium-Sulfur Batteries Based on Layered Double Hydroxides-Carbon Nanotubes Composite Cathode and a Dual-Functional Graphene-Polypropylene-Al<sub>2</sub>O<sub>3</sub> Separator. *Adv. Funct. Mater.*, 1704294:1704294, 2017.

192. Song, R., Fang, R., Wen, L., Shi, Y., Wang, S., Li, F., *et al.*, A trilayer separator with dual function for high performance lithium–sulfur batteries. *J. Power Sources*, 301, 179–186, 2016.
193. Sun, W., Ou, X., Yue, X., Yang, Y., Wang, Z., Rooney, D., *et al.*, A simply effective double-coating cathode with  $\text{MnO}_2$  nanosheets/graphene as functionalized interlayer for high performance lithium-sulfur batteries. *Electrochim. Acta*, 207, 198–206, 2016.
194. Shaibani, M., Hollenkamp, A.F., Hill, M.R., Majumder, M., Shaibani, M., *et al.*, Permselective membranes in lithium–sulfur batteries. *Curr. Opin. Chem. Eng.*, 16, 31–38, 2017.
195. Huang, J.-Q., Zhuang, T.-Z., Zhang, Q., Peng, H.-J., Chen, C.-M., Wei, F., *et al.*, Permselective Graphene Oxide Membrane for Highly Stable and Anti-Self-Discharge Lithium–Sulfur Batteries. *ACS Nano*, 9(3), 3002–3011, 2015.
196. Zhang, Y., Miao, L., Ning, J., Xiao, Z., Hao, L., Wang, B., *et al.*, A graphene-oxide-based thin coating on the separator: an efficient barrier towards high-stable lithium–sulfur batteries. *2D Mater.*, 2(2), 024013, 2015.
197. Xu, C., Shi, X., Ji, A., Shi, L., Zhou, C., Cui, Y., *et al.*, Fabrication and characteristics of reduced graphene oxide produced with different green reductants. *PLoS ONE*, 10(12), e0144842, 2015.
198. Zhu, P., Zang, J., Zhu, J., Lu, Y., Chen, C., Jiang, M., *et al.*, Effect of reduced graphene oxide reduction degree on the performance of polysulfide rejection in lithium-sulfur batteries. *Carbon N Y*, 126, 594–600, 2018.
199. Wang, X., Wang, Z., Chen, L., Reduced graphene oxide film as a shuttle-inhibiting interlayer in a lithium–sulfur battery. *J. Power Sources*, 242, 65–69, 2013.
200. Li, H., Sun, L., Zhang, Y., Tan, T., Wang, G., Bakenov, Z., *et al.*, Enhanced cycle performance of Li/S battery with the reduced graphene oxide/activated carbon functional interlayer. *Journal of Energy Chemistry*, 26(6), 1276–1281, 2017.
201. Dreyer, D.R., Park, S., Bielawski, C.W., Ruoff, R.S., Graphite oxide. *Chem. Soc. Rev.*, 2010.
202. Vizintin, A., Lozinšek, M., Chellappan, R.K., Foix, D., Krajnc, A., Mali, G., *et al.*, Fluorinated Reduced Graphene Oxide as an Interlayer in Li–S Batteries. *Chem. Mater.*, 27(20), 7070–7081, 2015.
203. Shin, W.-K., Kannan, A.G., Kim, D.-W., Effective Suppression of Dendritic Lithium Growth Using an Ultrathin Coating of Nitrogen and Sulfur Codoped Graphene Nanosheets on Polymer Separator for Lithium Metal Batteries. *ACS Appl. Mater. Interfaces*, 7(42), 23700–23707, 2015.
204. Ou, X., Yu, Y., Wu, R., Tyagi, A., Zhuang, M., Ding, Y., *et al.*, Shuttle Suppression by Polymer-Sealed Graphene-Coated Polypropylene Separator. *ACS Appl. Mater. Interfaces*, 10(6), 5534–5542, 2018.
205. Du, Z., Guo, C., Wang, L., Hu, A., Jin, S., Zhang, T., *et al.*, Atom-Thick Interlayer Made of CVD-Grown Graphene Film on Separator for Advanced

Lithium–Sulfur Batteries. *ACS Appl. Mater. Interfaces*, 9(50), 43696–43703, 2017.

- 206. Zhu, J., Chen, C., Lu, Y., Zang, J., Jiang, M., Kim, D., *et al.*, Highly porous polyacrylonitrile/graphene oxide membrane separator exhibiting excellent anti-self-discharge feature for high-performance lithium–sulfur batteries. *Carbon N Y*, 101, 272–280, 2016.
- 207. Zhuang, T.-Z., Huang, J.-Q., Peng, H.-J., He, L.-Y., Cheng, X.-B., Chen, C.-M., *et al.*, Rational Integration of Polypropylene/Graphene Oxide/Nafion as Ternary-Layered Separator to Retard the Shuttle of Polysulfides for Lithium-Sulfur Batteries. *Small*, 12(3), 381–389, 2016.
- 208. Xu, W., Wang, J., Ding, F., Chen, X., Nasybulin, E., Zhang, Y., *et al.*, Lithium metal anodes for rechargeable batteries. *Energy Environ. Sci.*, 7(2), 513–537, 2014.
- 209. Chen, K.-H., Wood, K.N., Kazyak, E., LePage, W.S., Davis, A.L., Sanchez, A.J., *et al.*, Dead lithium: mass transport effects on voltage, capacity, and failure of lithium metal anodes. *J. Mater. Chem. A*, 5(23), 11671–11681, 2017.
- 210. Wood, K.N., Kazyak, E., Chadwick, A.F., Chen, K.-H., Zhang, J.-G., Thornton, K., *et al.*, Dendrites and pits: Untangling the complex behavior of lithium metal anodes through operando video microscopy. *ACS Cent. Sci.*, 2(11), 790–801, 2016.
- 211. Zhang, Y.-jun., Xia, X.-hui., Wang, X.-li., Gu, C.-dong., Tu, J.-ping., *et al.*, Graphene oxide modified metallic lithium electrode and its electrochemical performances in lithium–sulfur full batteries and symmetric lithium–metal coin cells. *RSC Adv.*, 6(70), 66161–66168, 2016.
- 212. Bobnar, J., Lozinšek, M., Kapun, G., Njel, C., Dedryvère, R., Genorio, B., *et al.*, Fluorinated reduced graphene oxide as a protective layer on the metallic lithium for application in the high energy batteries. *Sci. Rep.*, 8(1), 5819, 2018.